Pharmaceutical Research, Vol. 26, No. 6, June 2009 (© 2009)
DOI: 10.1007/s11095-009-9849-7

Research Paper

The Role of Corneocytes in Skin Transport Revised—A Combined Computational and Experimental Approach

Steffi Hansen,[1] Arne Naegel,[2] Michael Heisig,[2] Gabriel Wittum,[2] Dirk Neumann,[3] Karl-Heinz Kostka,[4] Peter Meiers,[1] Claus-Michael Lehr,[1] and Ulrich F. Schaefer[1,5]

Received July 8, 2008; accepted February 6, 2009; published online February 25, 2009

Purpose. To investigate mechanisms of compound–corneocyte interactions in a combined experimental and theoretical approach.
Materials and Methods. Experimental methods are presented to investigate compound–corneocyte interactions in terms of dissolution within water of hydration and protein binding and to quantify the extent of the concurrent mechanisms. Results are presented for three compounds: caffeine, flufenamic acid, and testosterone. Two compartmental stratum corneum models M1 and M2 are formulated based on experimentally determined input parameters describing the affinity to lipid, proteins and water. M1 features a homogeneous protein compartment and considers protein interactions only via intra-corneocyte water. In M2 the protein compartment is sub-divided into a cornified envelope compartment interacting with inter-cellular lipids and a keratin compartment interacting with water.
Results. For the non-protein binding caffeine the impact of the aqueous compartment on stratum corneum partitioning is overestimated but is successfully modeled after introducing a bound water fraction that is non-accessible for compound dissolution. For lipophilic, keratin binding compounds (flufenamic acid, testosterone) only M2 correctly predicts a concentration dependence of stratum corneum partition coefficients.
Conclusions. Lipophilic and hydrophilic compounds interact with corneocytes. Interactions of lipophilic compounds are probably confined to the corneocyte surface. Interactions with intracellular keratin may be limited by their low aqueous solubility.

KEY WORDS: compartmental model; dual-sorption theory; Langmuir isotherm; partition coefficient; skin.

INTRODUCTION

In the pharmaceutical field of drug application it is well established that occlusion effectively enhances skin permeation of hydrophilic compounds by increasing the partitioning into the SC (1). This principle is used in occlusive semisolid formulations and transdermal patches. SC hydration may further vary due to patient skin type (seborhoic/sebostatic), exposure to sun, wind, cold, air-conditioning, chemicals or cosmetics among many others. However, there is an ongoing debate on the mechanisms involved in these effects. Especially the potential influence of compound–corneocyte interaction on permeation through human stratum corneum (SC) is under discussion. For small lipophilic molecules, interactions with keratin or other proteins are usually neglected as there is a common consent that transport occurs mainly via the intercellular lipids. For hydrophilic molecules, corneocytes may offer an additional pathway across the SC, such as

[1] Department of Biopharmaceutics and Pharmaceutical Technology, Saarland University, Campus A4 1, 66123 Saarbruecken, Germany.
[2] Goethe-Center for Scientific Computing, Goethe-University, Frankfurt, Germany.
[3] Center for Bioinformatics Saar, Saarland University, Saarbruecken, Germany.
[4] Department of Plastic and Hand Surgery, Caritas-Hospital, Lebach, Germany.
[5] To whom correspondence should be addressed. (e-mail: ufs@mx.uni-saarland.de)

ABBREVIATIONS: Aqu, aqueous corneocyte domain; c_i, concentration; $c_{max,i}$, Langmuir saturation constant (maximum binding capacity); CAF, caffeine; cor, corneocytes; cpe, cornified protein envelope; D_{cor}, diffusion coefficient within corneocytes; DCM, dichloro methane; don, Donor; FFA, flufenamic acid; SC,dry, usually freeze-dried SC, $\omega_{aqu}=0$; SC,hyd, hydrated SC; k_i, Langmuir binding affinity (adsorption coefficient); $K_{i/j}$, partition coefficient; $K_{Oct/w}$, logarithmical octanol water partition coefficient; ker, keratin; lip, intercellular SC lipid bilayers; LVP, low viscous paraffin; M1, compartmental model 1; M2, compartmental model 2; *MW*, molecular weight; pK_a, acid constant; pro, SC proteins (=ker+cpe); $q_{max,i}$, protein maximum loading capacity; s_i, saturation concentration; SC, stratum corneum; Soer,7.4, Soerensen phosphate buffer pH 7.4; TST, testosterone; V_i, volume; w_i, weight; w_0, weight of substance within the incubation solution before equilibration; w_{End}, weight of substance within the incubation solution after equilibration; ρ_i, density; $\Gamma_{i,j}$, interface; Ω_i, compartment; φ_j^i, volume fraction V_i/V_j; ω_j^i, weight fraction w_i/w_j; $\omega_{SC,dry}^{aqu,bound}$, weight fraction of bound aqueous phase per weight of dry SC.

through the controversially discussed continuous desmosome-corneocyte route (2–8). Meanwhile, there is significant evidence that the corneocytes are accessible for - at least a few - permeants. It is unquestionable that water enters the corneocytes very effectively (9,10). In addition, several larger hydrophilic and even lipophilic molecules (usually dyes) were visualized inside the corneocytes either by conventional or high speed two-photon microscopy (11,12). Boddé *et al.* found hints that disintegrating desmosomes serve as an entrance through the cornified envelope into the corneocytes in the apical SC (13). In the light of these results, the neglect of compound–corneocyte interaction is challenged. This is even more substantial for predictive models of SC permeability or SC flux.

The gain in knowledge about the SC structure and the permeant–barrier interaction is reflected in the development of increasingly sophisticated morphology based mathematical models for skin transport. In the simplest case, the SC morphology is approximated by a brick-and-mortar model with an inaccessible intra-cellular phase. Here, the corneocytes (bricks) simply serve as obstacles reducing diffusive area and increasing path length (14,15). Some of these models mimic the anisotropic structure of the SC lipid bilayers (16–19) by using anisotropic transport in lateral and trans-bilayer direction (14,15,20,21). Other elaborate models implement a trans-corneocyte pathway assuming a homogeneous interior and isotropic intra-cellular transport (21–26). Finally, Wang *et al.* used hindered diffusion theory to estimate the corneocyte diffusion coefficient D_{cor} in order to account for intra-corneocyte keratin forming fibrous obstacles (27–29).

Despite these obvious advances the available experimental data on compound–corneocyte interactions are still scarce and too inaccurate to validate morphologically exact diffusion models. For which substances do corneocyte interactions take place? Which structures are responsible for the interactions? Which compound properties are relevant for interactions with specific structural elements of the corneocytes? And finally, how could these be evaluated quantitatively?

Corneocytes are filled with a protein network of keratin intermediate filaments and are surrounded by a cornified protein envelope (cpe) (30). Together with small hydrophilic hygroscopic molecules—the natural moisturizing factors (*e.g.* urea, amino acids, and lactic acid)—keratin provides the major water holding capacity of the SC thus regulating skin flexibility, firmness, and smoothness. Hence, water present in healthy skin *in vivo*, *i.e.* about 15–30% per weight of dry SC (31) is tightly bound (32–34). Through occlusion or in a very humid environment additional water (up to several times the weight of the dry tissue) may be taken up by the corneocytes. Finally, water intercalates between intercellular lipids to occasionally form water pools of vesicle-like structure but without causing any major disruption of the lipid bilayers (35,36). Corneodesmosomes mediate cellular contact between adjacent corneocytes and provide SC cohesion until they are gradually degraded during desquamation within the stratum disjunctum. In summary, interactions of a penetrating molecule with the SC are possible with (1) intercellular lipids; (2) keratin and proteins of the corneodesmosomes or the cornified protein envelope; (3) water.

The primary interaction of a compound with intercellular lipids or water is dissolution of the substance in the liquid phase. At equilibrium, the ratio of concentrations between two adjacent non-miscible media, is determined by the partition coefficient, *i.e.* the ratio of solubility in both phases. In contrast, small molecules interact with proteins by forming complexes. In simple cases, the number of protein-bound molecules may be calculated from a Langmuir isotherm. For concentrations far away from saturation of binding sites the relationship between free and bound concentration is sufficiently described by a linear relationship, *i.e.* in terms of a partition coefficient. Approaching saturation the concentration of bound substance becomes independent of free concentration visible as a plateau.

Previous models that take into account the anatomical heterogeneity of SC in detail assume that interactions with the protein phase are regulated by a partition coefficient (37,38). These apply in the limit that compound concentrations are low and far away from saturation. However, non-linear concentration influences indicating saturable processes are being repeatedly reported in literature. These include binding studies using isolated keratin protein (39,40) as well as SC-donor partition coefficients ($K_{SC/don}$) of a number of compounds (such as doxycyclin (39), primaquine (40), timolol (41), testosterone, hydrocortisone, estradiol, progesterone (42), cyanophenol, iodophenol, and pentyloxyphenol (43)). Even for studies where no non-linear concentration dependence is reported (43–45) this may be an effect of a low protein binding constant or that potential protein binding compounds are denied access to the binding sites, as for example keratin is mainly found intra-cellular. The same effect would be caused by an insufficient compound solubility in the surrounding tissue as then the maximum binding capacity cannot be achieved. The non-linear development of the binding isotherm may further be overcompensated by non-saturable partitioning. This concept has first been introduced for the adsorption of gases to glassy polymers as the "dual sorption"-theory but may be ubiquitously applied to processes with concurrent mobile and fixed species of the same compound irrespective of the mechanism of immobilization (46). Chandrasekaran *et al.* transferred the concept to the interaction with human epidermal membranes and SC using the example of scopolamine (47). They described the process as a combination of dissolution creating mobile, freely diffusible molecules and adsorption producing non-mobile molecules that cannot contribute to the diffusion process (47). Between mobile and non-mobile species a rapid exchange compared to the diffusion time-scale and a local equilibrium is assumed. The authors however assumed the whole membrane to participate in dissolution and binding of drug molecules. The aim is now to relate mobile and fixed drug species to specific SC substructures.

Lately we established experimental methods to quantify the tendency of compounds to interact with the corneocytes in terms of a corneocyte-intercellular lipids partition coefficient ($K_{cor/lip}$) (48). Although this method provides a general idea of the overall extent of corneocyte uptake, it does not allow insight into the mechanism of interaction. The question is how to analyze the contributions of the individual structural elements of the SC experimentally. Techniques have been reported how to adopt equilibration experiments so as to determine a compound's affinity to SC lipids. However, to our knowledge only two data-sets of experimentally measured partition coefficients into extracted SC lipids are reported for a very limited set of compounds. These are a series of 11 hydrocortisone esters from Raykar *et al.* and caffeine (CAF) and flufenamic acid (FFA) from our own

works (37,48). Usually this problem is circumvented by employing a correlation between the lipid-donor partition coefficient ($K_{lip/don}$) and the octanol–water partition coefficient ($K_{Oct/w}$) according to a power law (linear free energy relationship) (14,38,49).

Similar correlations have also been proposed to exist between the corneocytes–water partition coefficient ($K_{cor/w}$) and $K_{Oct/w}$ (37,38,50,51). Furthermore, partition coefficients into delipidized SC and callus shavings have been proposed as a model to investigate compound binding to corneocyte proteins (37,42,52). There are several shortcomings of these methods. Lipid extraction with methanol/chloroform cannot remove the ω-OH-acylceramides covalently attached to the cpe (53). This may lead to an overestimation of protein binding of lipophilic compounds. Treatment with organic solvents will denature the corneocyte proteins so that binding properties will most probably be very different from intact SC. Finally, like intact SC delipidized SC and callus will hydrate significantly during incubation with aqueous media so that again it is not obvious whether substance uptake is due to protein binding or dissolution in the corneocyte water phase. These shortcomings may be overcome by using isolated pulverized animal keratin instead. Binding studies using keratin from bovine hoof and horn have been done in the past with a focus on fungicides and anti-malaria drugs (39,40,54,55). The pattern of keratin proteins depends on species, tissues, as well as states of terminal differentiation (56,57). The amino acid composition of human and bovine epidermal keratins is relatively comparable which most probably reflects identical function (58).

Uptake into aqueous SC domains has so far only been investigated indirectly by comparing SC-water partition coefficients estimated from the decrease of the donor concentration (method 1) and from the extraction of the SC after equilibrium (method 2) (37). This method is based on the assumption that the dissolution properties of water inside the SC are identical to bulk water. Recently, it was shown that significant portions of water are tightly bound to SC structures and are therefore unavailable for compound dissolution (32–34). Ignoring bound water leads to wrong estimates of $K_{SC/don}$ according to method 1 and therefore of the uptake into aqueous domains of the SC (59,60). The aim is now to investigate partitioning into aqueous stratum corneum domains directly by measuring $K_{SC/don}$ at clearly defined hydration levels. This will be possible by switching to a non-aqueous donor such as low viscous paraffin (LVP) to avoid the uncontrolled excessive hydration that happens with an aqueous donor. SC may now be used dry or gradually hydrated and a series of equilibration experiments may be performed with SC of known water content as displayed in Fig. 1. At zero hydration the SC-LVP partition coefficient ($K_{SC/LVP}$) will exclusively be determined by the intercellular lipids and accessible proteins (Fig. 1B). With increasing hydration $K_{SC/LVP}$ should be influenced depending on the affinity of the molecule to water if the aqueous domain is accessible for drug molecules (Fig. 1C). By measuring $K_{SC/LVP}$ at different hydration levels it can be tested whether water uptake has a linear influence on $K_{SC/LVP}$ indicative of a partitioning process.

We could recently show that corneocyte interactions need to be taken into account for both the hydrophilic caffeine (CAF; $\log K_{Oct/w}$ −0.08) and the lipophilic flufenamic acid (FFA; $\log K_{Oct/w}$ 4.8) (48). In the case of FFA, keratin binding had been suspected to be responsible for the observed corneocyte interaction while this could be ruled out for CAF (48). Apart from that dissolution within the aqueous corneocyte domain is imaginable for both compounds CAF being highly soluble in water and FFA being a weak acid exhibiting a pH dependent aqueous solubility (pK_a 3.8; (61)). Naegel and coworkers demonstrated the significance of the corneocyte involvement for the shape of the SC concentration-depth profiles of both FFA and CAF through numerical modeling on the basis of experimental input values on all relevant partition and diffusion coefficients (23). For both compounds their mechanism of corneocyte interaction shall now be clarified. The original set of compounds has been extended by testosterone (TST; $\log K_{Oct/w}$ 3.32) as it is practically insoluble in water but stands a good chance to bind to keratin due to its high lipophilicity. TST is in contrast to FFA non-ionizable and therefore its aqueous solubility is independent of pH. In addition, CAF and TST are typical examples of reference compounds recommend by the internationally accepted guidelines 427 and 428 of the Organization for Economic Cooperation and Development (OECD) for performing system suitability tests for skin permeation experiments (62,63). For all three compounds $K_{SC/LVP}$ was measured as a function of SC hydration and donor concentration.

In order to interpret the experimental results quantitatively two constitutive compartmental models of SC are formulated. These allow an easy prediction of $K_{SC/don}$ as a function of membrane composition, in detail SC hydration, and donor concentration. The spatial resolution is given by the compartments that are defined and is limited by the degree to which reliable estimates of input parameters are available. To quantify compound interactions with individual compartments the two elements of the "dual-sorption"-theory (47), *i.e.* non-saturable dissolution and saturable binding were applied to individual compartments in terms of partition coefficients and Langmuir binding isotherms. Input data was either experimentally derived or found in theoretical parameter studies. Calculations are evaluated by comparing results with independently determined experimental $K_{SC/LVP}$. Discrepancies between measurements and predictions are investigated by systematically varying critical input parameters.

THEORY

Definition of Compartments and Interfaces

We assume a compartmental composition of the SC of lipids and corneocytes, Ω_{lip} and Ω_{cor}. Two main states of the SC will be discussed. These are "hydrated SC" (SC,hyd) and "dry SC" (SC,dry). The latter is an artificial state obtained by freeze-drying of excised SC which is only relevant for the *in vitro* situation. Nonetheless, it will be useful for illustrating the effect of SC water content and protein binding. "SC,dry" is composed of a lipid and a protein compartment

$$\Omega_{SC,dry} = \Omega_{lip} + \Omega_{pro} \quad (1)$$

"SC,hyd" additionally contains an aqueous compartment

$$\Omega_{SC,hyd} = \Omega_{SC,dry} + \Omega_{aqu} \quad (2)$$

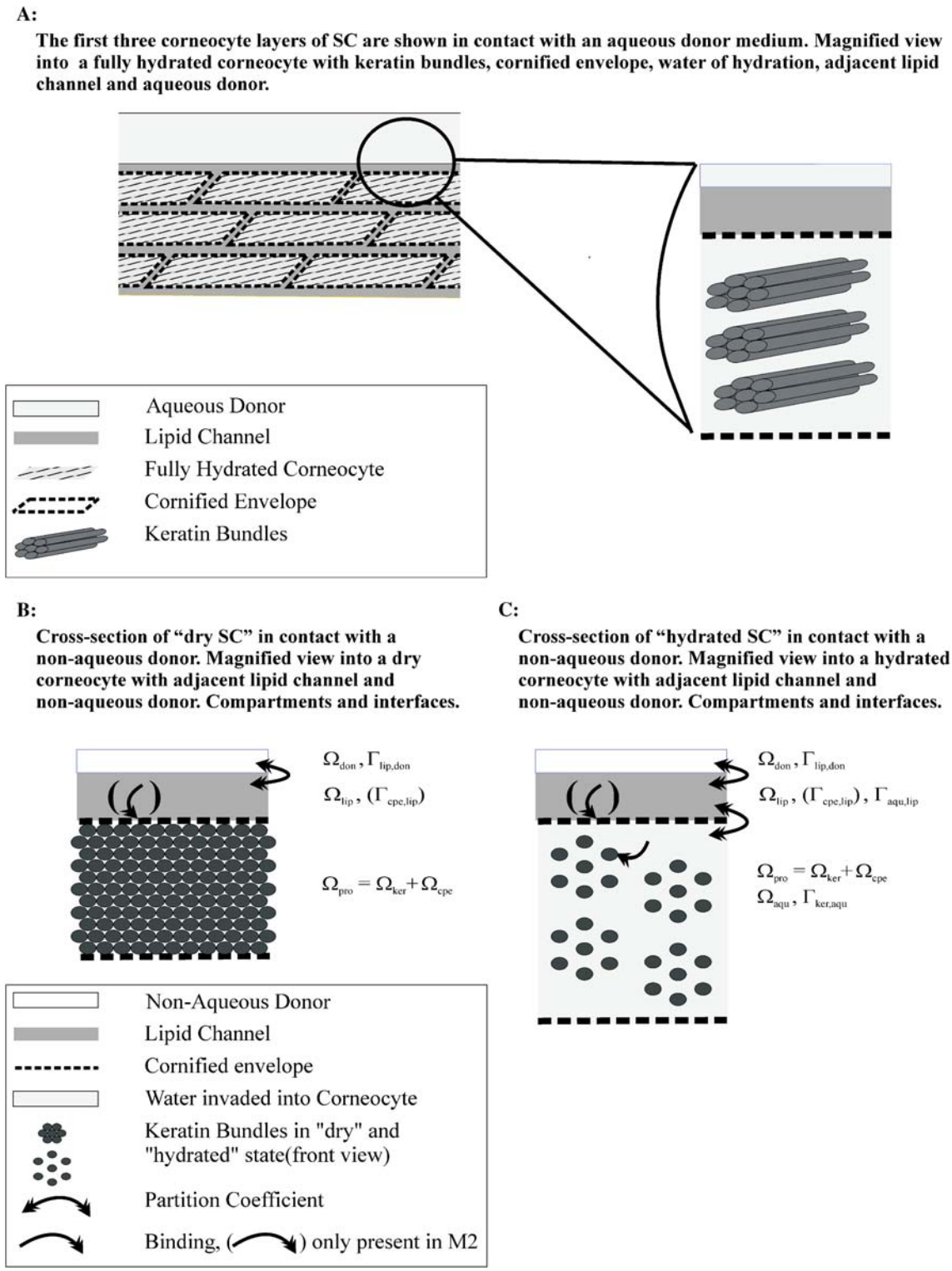

Fig. 1. **A** Upon contact with an aqueous donor water invades into the corneocytes. **B**, **C** Incubating excised SC with a non-aqueous donor such as low viscous paraffin allows working at a defined hydration state. Compartments and interfaces used in the compartmental models of "dry SC" (**B**) and "hydrated SC" (**C**). Not drawn to scale.

Such a compartmental composition in dry and hydrated state will be discussed as "Model 1" (M1). As an extension of M1, Ω_{pro} will be further subdivided into a keratin and a cornified envelope sub-compartment in "Model 2" (M2)

$$\Omega_{pro} = \Omega_{ker} + \Omega_{cpe} \tag{3}$$

The membrane is in contact with an inert donor medium Ω_{don}. Adjacent compartments are separated by interfaces $\Gamma_{lip,don}$, $\Gamma_{aqu,lip}$, $\Gamma_{pro,lip}$, and $\Gamma_{pro,aqu}$ in M1 and $\Gamma_{lip,don}$, $\Gamma_{aqu,lip}$, $\Gamma_{ker,aqu}$, and $\Gamma_{cpe,lip}$ in M2. By definition Ω_{aqu} and Ω_{cpe} do not share a common interface. The theoretical interface $\Gamma_{cpe,ker}$ is ignored as direct substance exchange between two solids is considered impossible. An index set I={don,lip,aqu,pro,ker,cpe} will be used to avoid unnecessary abundant notation. Compartments and interfaces are then referred to by the symbol Ω_i and $\Gamma_{i,j}$ for $i \neq j$ and $i, j \in$ I (Table I). The composition of the model membrane with the described compartments and interfaces at dry and hydrated state is depicted in Fig. 1.

Description of Compound Membrane Interaction

M1 and M2 apply to equilibrium conditions. We consider the whole SC volume accessible for compounds which is expressed in the following set of equations for M1 (Eqs. 4 and 5) and M2 (Eqs. 6 and 7) at dry and hydrated state

$$c_{SC,dry} = \varphi^{lip}_{SC,dry} c_{lip} + \varphi^{pro}_{SC,dry} c_{pro} \tag{4}$$

$$c_{SC,hyd} = \varphi^{lip}_{SC,hyd} c_{lip} + \varphi^{pro}_{SC,hyd} c_{pro} + \varphi^{aqu}_{SC,hyd} c_{aqu} \tag{5}$$

$$c_{SC,dry} = \varphi^{lip}_{SC,dry} c_{lip} + \varphi^{ker}_{SC,dry} c_{ker} + \varphi^{cpe}_{SC,dry} c_{cpe} \tag{6}$$

$$c_{SC,hyd} = \varphi^{lip}_{SC,hyd} c_{lip} + \varphi^{ker}_{SC,hyd} c_{ker} + \varphi^{cpe}_{SC,hyd} c_{cpe} + \varphi^{aqu}_{SC,hyd} c_{aqu} \tag{7}$$

with the concentration of a substance within a compartment being defined as $c_i = w/V_i$, *i.e.* as the weight of the substance in the compartment relative to its volume. The volume fractions of the compartments relatively to the volume of the SC are defined as $\varphi^i_{SC} = V_i/V_{SC}$. Although substantial portions of water are known to be tightly bound to proteins as a starting point we assume all water to be available for compound dissolution. This is in agreement with SC partitioning experiments performed with sucrose by Raykar *et al.* who could not find proof of an inaccessible water fraction within human SC (37).

Substance-compartment interactions are modelled depending on the nature of the compartment. At $\Gamma_{lip,don}$ and $\Gamma_{aqu,lip}$ partition coefficients $K_{i/j}$ are applied. That is:

$$c_i(x) = K_{i/j} c_j(x) \tag{8}$$

holds for $x \in \Gamma_{i,j}$, with $(i, j) \in \{(lip, don), (aqu, lip)\}$.

For all protein compartments Ω_{pro}, Ω_{ker}, and Ω_{cpe} we follow the rationale by Chandrasekaran *et al.* who suggested a non-linear dependence assuming a limited number of available binding sites and described the relationship between protein-bound and free concentration by a Langmuir-isotherm (47)

$$c_i(x) = \frac{k_i c_{max,i} c_j(x)}{1 + k_i c_j(x)} \tag{9}$$

for $x \in \Gamma_{i,j}$, with $(i, j) = (pro, aqu)$ for M1 and $(i, j) \in \{(ker, aqu), (cpe, lip)\}$ for M2. In this sense for M1 we assume $\Gamma_{pro,lip}$ to be an "inert" interface and protein binding only via $\Gamma_{pro,aqu}$. Due to the coupling of Ω_{aqu}, Ω_{lip}, and Ω_{don} via $K_{aqu/lip}$ and $K_{lip/don}$ at $\Gamma_{aqu,lip}$ and $\Gamma_{lip,don}$ the free (and thus also the bound) concentrations will be a function of c_{don}:

$$c_{aqu} = K_{aqu/lip} c_{lip} = K_{aqu,lip} K_{lip/don} c_{don} = K_{aqu/don} c_{don} \tag{10}$$

$$c_{lip} = K_{lip/don} c_{don} \tag{11}$$

From an anatomical standpoint direct lipid-protein contact can only reasonably be assumed between SC lipids and the cpe or corneodesmosomes. As a first approach in M2 we are concentrating on the cpe for the simple reason that information on its dimensions are available from literature (30).

This has severe consequences for the description of c_{SC}. For M1 the concentration within "SC,dry" and "SC,hyd" are given by

$$c_{SC,dry} = \varphi^{lip}_{SC,hyd} K_{lip/don} c_{don} \tag{12}$$

Table I. Compartments and Interfaces of the Model Membrane in M1 and M2

Compartments and interfaces	Symbols	Partition coefficients and binding constants	Concentrations	Model
Donor compartment	Ω_{don}		c_{don}	M1
Interface	$\Gamma_{lip,don}$	$K_{lip/don}$		SC,dry
Lipid layers	Ω_{lip}		c_{lip}	
Interfaces	$\Gamma_{pro,lip}$	no interaction		
	$\Gamma_{aqu,lip}$	$K_{aqu/lip}$		M1
Aqueous compartment	Ω_{aqu}		c_{aqu}	SC,hyd
Interface	$\Gamma_{pro,aqu}$	k_{pro} and $c_{max,pro}$		
Protein compartment	Ω_{pro}		c_{pro}	
Donor compartment	Ω_{don}		c_{don}	M2
Interface	$\Gamma_{lip,don}$	$K_{lip/don}$		SC,dry
Lipid layers	Ω_{lip}		c_{lip}	
Interfaces	$\Gamma_{aqu,lip}$ and $\Gamma_{cpe,lip}$	$K_{aqu/lip}$, k_{cpe} and $c_{max,cpe}$		
Cornified envelope compartment	Ω_{cpe}		c_{cpe}	M2
Aqueous compartment	Ω_{aqu}		c_{aqu}	SC,hyd
Interface	$\Gamma_{ker,aqu}$	k_{ker} and $c_{max,ker}$		
Keratin compartment	Ω_{ker}		c_{ker}	

as $\Omega_{aqu}=\emptyset$, and consequently $c_{aqu}=c_{pro}=0$, and by

$$c_{SC,hyd} = \varphi^{lip}_{SC,hyd} K_{lip/don} c_{don} + \varphi^{pro}_{SC,hyd} \frac{k_{pro} c_{max,pro} K_{aqu/don} c_{don}}{1 + k_{pro} K_{aqu/don} c_{don}} + \varphi^{aqu}_{SC,hyd} K_{aqu/don} c_{don} \quad (13)$$

For M2 $c_{SC,dry}$ and $c_{SC,hyd}$ are described as

$$c_{SC,dry} = \varphi^{lip}_{SC,dry} K_{lip/don} c_{don} + \varphi^{cpe}_{SC,dry} \frac{k_{cpe} c_{max,cpe} K_{lip/don} c_{don}}{1 + k_{cpe} K_{lip/don} c_{don}} \quad (14)$$

as $\Omega_{aqu}=\emptyset$, $c_{aqu}=c_{ker}=0$ and by

$$c_{SC,hyd} = \varphi^{lip}_{SC,hyd} K_{lip,don} c_{don} + \varphi^{ker}_{SC,hyd} \frac{k_{ker} c_{max,ker} K_{aqu,don} c_{don}}{1 + k_{ker} K_{aqu,don} c_{don}} + \varphi^{cpe}_{SC,hyd} \frac{k_{cpe} c_{max,cpe} K_{lip,don} c_{don}}{1 + k_{cpe} K_{lip,don} c_{don}} + \varphi^{aqu}_{SC,hyd} K_{aqu,don} c_{don} \quad (15)$$

Note that in Eq. 9 $c_i(x)$ depends only on the concentration $c_j(x)$ but not on the volume fraction φ^j_{SC} . In other words, at high SC hydration water intercalates between lipids so that parts of Ω_{aqu} share no interface with Ω_{pro} or Ω_{cpe}. Nonetheless the bound concentration will still be correctly described by Eq. 9. This is of course only true if the number of binding sites is independent of φ^{aqu}_{SC} .

The Special Case of Non-protein Binding Substances

In the special case of non-protein binding substances, the maximum concentrations $c_{max,i}$ are identically zero. Therefore, the terms corresponding to the Langmuir isotherms vanish and, for both M1 and M2, the same result is obtained for $c_{SC,dry}$ (Eq. 12) and $c_{SC,hyd}$

$$c_{SC,hyd} = \varphi^{lip}_{SC,hyd} K_{lip,don} c_{don} + \varphi^{aqu}_{SC,hyd} K_{aqu,don} c_{don} \quad (16)$$

respectively.

Calculation of a Theoretical Stratum Corneum-Donor Partition Coefficient

The theoretical SC-donor partition coefficient is calculated by applying Eq. 8 to the whole SC membrane and rearranging for $K_{SC/don}$

$$K_{SC/don} = \frac{c_{SC}}{c_{don}} \quad (17)$$

Accordingly, in Eqs. 5, 6, 7, 8, and 9 c_{SC} is divided by c_{don} to calculate $K_{SC,hyd}$ and $K_{SC,dry}$ for M1 (Eqs. 18 and 19), M2 (Eqs. 20 and 21) and non-keratin binding substances (Eq. 22).

$$K_{SC,dry/don} = \varphi^{lip}_{SC,dry} K_{lip/don} \quad (18)$$

$$K_{SC,hyd/don} = \varphi^{lip}_{SC,hyd} K_{lip/don} + \varphi^{pro}_{SC,hyd} \frac{k_{pro} c_{max,pro} K_{aqu/don}}{1 + k_{pro} K_{aqu/don} c_{don}} + \varphi^{aqu}_{SC,hyd} K_{aqu/don} \quad (19)$$

$$K_{SC,dry/don} = \varphi^{lip}_{SC,dry} K_{lip/don} + \varphi^{cpe}_{SC,dry} \frac{k_{cpe} c_{max,cper} K_{lip/don}}{1 + k_{cpe} K_{lip/don} c_{don}} \quad (20)$$

$$K_{SC,hyd/don} = \varphi^{lip}_{SC,hyd} K_{lip/don} + \varphi^{ker}_{SC,hyd} \frac{k_{ker} c_{max,ker} K_{aqu/don}}{1 + k_{ker} K_{aqu/don} c_{don}} + \varphi^{cpe}_{SC,hyd} \frac{k_{cpe} c_{max,cpe} K_{lip/don}}{1 + k_{cpe} K_{lip/don} c_{don}} + \varphi^{aqu}_{SC,hyd} K_{aqu/don} \quad (21)$$

$$K_{SC,hyd/don} = \varphi^{lip}_{SC,hyd} K_{lip,don} + \varphi^{aqu}_{SC,hyd} K_{aqu,don} \quad (22)$$

In order to compare calculated with experimental results, values of $K_{SC,hyd/don}$ need to be transformed to $K_{SC,dry/don}$ via (for the derivation see Appendix B):

$$K_{SC,dry/don} = \frac{K_{SC,hyd/don}}{\varphi^{SC,dry}_{SC,hyd}} \quad (23)$$

Input Parameters

The following paragraph relates the terms in Eqs. 18, 19, 20, 21 and 22 to experimentally measured parameters for the special case of LVP as donor medium and for CAF, FFA, and TST as model compounds.

The Stratum Corneum Lipid-low Viscous Paraffin Partition Coefficient $K_{lip/LVP}$

According to the definition of the partition coefficient in Eq. 8 the upper limit is determined by the ratio of the saturation concentrations within the two phases (s_i and s_j). In this sense $K_{lip/LVP}$ can be expressed as in Eq. 24. In an earlier publication for CAF and FFA we measured $K_{lip/don}$ for don being Soerensen phosphate buffer pH 7.4 (Soer,7.4) (Eq. 25) (48). Rearranging Eq. 25 for s_{lip} and substituting it into Eq. 24 $K_{lip/LVP}$ is calculated from the measured quantities $K_{lip/Soer,7.4}$, $s_{Soer,7.4}$, and s_{LVP} (Eq. 26).

$$K_{lip/LVP} = \frac{s_{lip}}{s_{LVP}} \quad (24)$$

$$K_{lip/Soer,7.4} = \frac{s_{lip}}{s_{Soer,7.4}} \quad (25)$$

$$K_{lip/LVP} = \frac{K_{lip/Soer,7.4} s_{Soer,7.4}}{s_{LVP}} \quad (26)$$

For TST no experimental data on $K_{lip/Soer,7.4}$ were available so that first the lipid–water partition coefficient $K_{lip/w}$ was inferred from the octanol–water partition coefficient $K_{Oct/w}$ as proposed in (38) (Eq. 27). The aqueous solubility of TST being pH independent, $K_{lip/w}$ was taken to be identical to $K_{lip/Soer,7.4}$ so that $K_{lip/LVP}$ could then be calculated according to Eq. 26.

$$K_{lip/w} = \left(K_{Oct/w}\right)^{0.78} \tag{27}$$

Equation 27 is subject to uncertainty as it relies on a fitting procedure and depends on the diversity and accuracy of the underlying database. A number of similar correlations of the general form

$$K_{lip/w} = aK_{Oct/w}^{b} \tag{28}$$

have been proposed. Taking $a=1$ values for b were suggested in the range of 0.70 to 0.78 (38,49,64–66). Considering both a and b as being variable, values as high as 0.91 have been suggested for b (37). The exponent of 0.78 was chosen because it was derived for a database of experimentally determined SC lipid–water partition coefficients. A comparison of calculated values of $K_{lip/w}$ for CAF and FFA with experimentally determined values shall serve as a test of consistency of estimates of Eq. 27. For CAF and FFA Eq. 27 predicts $K_{lip/w}$ to be 0.87 and 38.37 while experimental values were 2.15±0.42 and 20.32±0.54 respectively (note that for FFA the prediction was corrected for pH 7.4 as this was used in the experiment (48)). Despite the experimental and theoretical uncertainty Eq. 27 seems to be a valuable instrument to estimate $K_{lip/w}$ for TST where no experimental results are available.

The Aqueous Compartment-low Viscous Paraffin Partition Coefficient $K_{aqu/LVP}$

$K_{aqu/LVP}$ was calculated for CAF, FFA, and TST as proposed for $K_{lip/LVP}$ from the saturation concentrations in aqu and LVP. The solvent properties of aqu were supposed to be essentially like bulk water. For CAF and TST the aqueous solubility is independent of pH so that $s_{Soer,7.4}$ seems a reasonable experimental approximation for s_{aqu}. In contrast for FFA a pH correction was necessary. Depending on the analytical method opinions on corneocyte pH vary ranging from moderately acidic (pH 5.5–6.5; employing surface parallel pH electrodes combined with tape-stripping (67)) to practically neutral (measuring the fluorescence lifetime of pH-sensitive dyes, *e.g.* 2′,7′-bis-(2-carboxyethyl)-5-(and-6)-carboxyfluorescein (68)). Due to the lipophilicity of the fluorescent dye the latter method exclusively probes the intercellular lipid channel while information on the corneocyte pH is most probably not available. Therefore 5.5 and 6.5 seem a reasonable estimate for the lower and upper margin of the corneocyte pH. Accordingly the lower margin of $K_{aqu/LVP}$ was calculated for FFA using $s_{Soer,5.5}$ and the upper margin of $K_{aqu/LVP}$ was calculated using $s_{Soer,6.5}$. All analyses for FFA were performed for both pH-values.

The Langmuir Isotherm Describing Keratin Binding

In M1 the binding properties of the protein compartment will simplistically be described as keratin. Experimental data on $q_{max,ker}$ and k_{ker} measured with keratin from bovine hoof and horn is available from literature for CAF and FFA (48) or presented here for TST. The maximum binding capacity of a protein is usually reported in terms of its loading $q_{max,i}$, *i.e.* as a weight fraction relative to the weight of the protein (w/w) rather than as a concentration $c_{max,i}$ relative to the volume of the protein (w/V). $q_{max,i}$ is related to $c_{max,i}$ via the protein density:

$$c_{max,ker} = \frac{w}{V_{ker}} = \frac{w}{w_{ker}}\rho_{ker} = q_{max,ker}\rho_{ker} \tag{29}$$

It has been argued that with swelling keratin uncoils and exposes additional binding sites (69). Reported values for $q_{max,ker}$ and k_{ker} correspond to maximally expanded keratin as experiments were performed in "Soer,7.4". This might be a source for errors in the case of "dry SC". This is avoided by restricting keratin binding to be only possible in hydrated SC.

The Langmuir Isotherm Describing Binding to The Cornified Protein Envelope

In M2 binding to SC proteins is subdivided into binding to intra-cellular keratin accessible (as in M1) only from the aqueous compartment and binding to the cpe accessible only from the lipid compartment. For $q_{max,ker}$ and k_{ker} experimental data is readily available. In contrast there are no studies reporting the maximum binding capacity $q_{max,cpe}$ or the binding constant k_{cpe} to the cpe. Therefore we performed a theoretical parameter study where different combinations of $q_{max,cpe}$ (1, 10, 50, and 100 µg/mg) and k_{cpe} (10^{-3} ml/µg and 10^{3} ml/µg) were tested. Although these values are arbitrarily founded, they may serve to illustrate the potential of protein binding via the SC lipids in a range of possible protein binding constants and binding capacities.

MATERIAL AND METHODS

Material

The following materials and equipment were used: dialysis membrane MW-cut-off 25 kDa (Medicell International Ltd, London, Great Britain, VWR Darmstadt, Germany); Centrisart I cut-off 20 kDa (Sartorius AG, Goettingen, Germany); scintillation vials borosilicate glass with screw cap (VWR, Darmstadt, Germany); freeze-dryer (Alpha 2–4 LSC, Christ, Osterode, Germany); UV/VIS spectrophotometer (Lambda 35, Perkin Elmer, Rodgau-Jürgesheim, Germany); Hellma® precision cells made of Quartz SUPRASIL®, type 100-QS-10 (Hellma®, Muehlheim, Germany).

Chemicals

4-Androsten-17ß-ol-3-one (*i.e.* testosterone), flufenamic acid, caffeine, sodium chloride, potassium chloride, methanol, a bicinchoninic acid kit for protein determination, and Trypsin type I from bovine pancreas were supplied by Sigma Aldrich GmbH, Steinheim, Germany. Acetonitrile and sodium monohydrogen phosphate dihydrate were supplied by Fluka Chemie AG, Buchs, Germany. Low viscous paraffin (density at 20°C 0.818–0.875 g/cm^3; dynamic viscosity 25–80 mPas), citric acid monohydrate, potassium dihydrogen phosphate, orthophosphoric acid were supplied by Merck, Darmstadt, Germany. Keratin from bovine hoof and horn was supplied by ICN biomedicals, Aurora, Ohio.

Composition of Buffers

All buffer substances were of analytical grade and were prepared with purified water.

Phosphate buffered saline (PBS) pH 7.4: 1 l contains $Na_2HPO_4{\cdot}2H_2O$ 1.44 g, KH_2PO_4 0.2 g, NaCl 8 g, KCl 0.2 g.

Soerensen phosphate buffer: is composed of x parts 0.15 M Na_2HPO_4, and $100-x$ parts 0.15 M KH_2PO_4 (pH 5.5: $x=3.5$; pH 6.5: $x=30$; pH 7.4: $x=80.3$).

Buffer pH 2.2: 1 l contains citric acid monohydrate 20.8 g, $Na_2HPO_4{\cdot}2H_2O$ 0.4 g.

Buffer pH 2.6: 1 l contains orthophosphoric acid 1.16 ml, KH_2PO_4 2.04 g.

Skin Samples and Skin Preparation Techniques

Skin samples were taken from Caucasian female donors undergoing abdominal surgery with the approval of the ethic committee of the Caritas-Hospital Lebach, Germany. After removal of subcutaneous fatty tissue full thickness skin was stored at −26°C for a maximum of 6 months after surgery. For details see Wagner *et al.* (70).

Preparation of Stratum Corneum Sheets

SC sheets were prepared according to the method of Kligman and Christophers (71) by two times 24 h immersion of cleaned full thickness skin pieces of approximately 12 cm^2 in 0.15% (*w*/*V*) trypsine in PBS. In between as well as afterwards the pieces were washed three times with PBS and finally freeze-dried. Samples were kept at −26°C overnight to guarantee complete freezing and then equilibrated inside the single chamber system at −40°C. Main drying was performed overnight at 0.050 mbar, with a shelf temperature of 20°C and a condenser temperature of −80°C. For the final drying for 2 h the vacuum was elevated to 0.001 mbar keeping shelf and condenser temperature as during main drying. During the entire procedure the temperature of condenser and shelf was permanently monitored. Dried SC samples had a parchment like, crumply and brittle appearance. Freeze-dried membranes were kept in a freezer at −18°C for a maximum of 6 months after surgery.

Preparation of Hydrated Stratum Corneum

A gradual hydration of SC sheets was achieved by equilibrating freeze-dried SC sheets of known weight over a 15.32% *w*/*w* sodium chloride solution or pure water or immersion in water for 24 h at 32°C in desiccators. The hydrated SC sheets were weighed again (in the case of SC sheets immersed in water these were blotted dry between paper filters before weighing). The level of hydration was calculated as follows: % $w/w = 100\times$ (weight hydrated SC − weight dried SC)/weight dried SC.

Determination of Saturation Concentration

An excess of CAF, FFA or TST was suspended in 5 ml Soerensen buffer pH 5.5; 6.5; 7.4 or LVP in a screw top scintillation vial. The lid was secured with a Teflon disk. The mixture was stirred at 500 rpm at 32°C for at least 24 h. Stirring was stopped and the samples were further kept at 32°C until non-dissolved substance had settled down completely. Samples were drawn from the supernatant without disturbing the sediment and centrifuged for 5 min at 2795 g. During centrifugation the temperature of the samples did not change. The samples were diluted to an appropriate concentration and analyzed via HPLC or UV spectroscopy. Preliminary experiments had shown that saturation was complete within 24 h and no filtration was needed.

Keratin Binding

Prior to the experiment water soluble low molecular weight keratin fractions resulting from the manufacturing process were removed by classical dialysis using dialysis tubing with a molecular weight cut-off of 25 kDa. Removal of soluble keratin fraction was considered to be complete if a BCA-assay in the supernatant performed according to the standard protocol provided by the manufacturer was negative (linear concentration range 0.2–1 mg/ml or 5–25 µg of total protein, detection limit 0.01 µg/ml). Insoluble keratin fractions were retrieved by freeze-drying (for the freeze-drying procedure please refer to "Preparation of Hydrated Stratum Corneum").

Increasing ratios of TST to keratin (11 steps in the range of 0.025–4.68 µg/mg keratin using Soerensen buffer pH 7.4 as medium) were incubated on a magnetic stirrer (500 rpm) at 32°C, over 24 h, *i.e.* until equilibration. 1.0 ml of the suspension were transferred to centrisart tubes (MW-cut-off 20 kDa) and centrifuged for 20 min at 2,795×*g* at 25°C. The supernatant was diluted with Soerensen buffer pH 7.4 to an appropriate concentration and transferred into HPLC vials and the concentration of unbound substance was determined by HPLC. Samples containing only substance solution without keratin were subjected to the identical procedure and represented 100% free concentration.

Determination of Partition Coefficients by Equilibration Experiments

The substance concentration within the SC was determined from the decrease of the substance weight within the donor volume during incubation and normalized to the dry volume of SC where w_0 and w_{End} are the substance weight within LVP before and after equilibration

$$K_{SC,dry/don} = \frac{(w_0 - w_{End})/V_{SC,dry}}{w_{End}/V_{LVP}} \tag{30}$$

$V_{SC,dry}$ was determined from weighing freeze-dried SC by normalizing to the density of dry SC: 1.3 g/cm^3 (72).

Influence of Concentration of Incubation Solution

$K_{SC/don}$ was measured based on the equilibration method introduced by Raykar *et al.* (37). The concentration dependence of $K_{SC/don}$ was evaluated in a broad concentration range with dry$^{(d)}$ SC and for the "hydrated state" with SC hydrated over pure water$^{(h)}$ and additionally for exemplary concentrations for SC hydrated above sodium chloride$^{(NaCl)}$ and by bathing in water$^{(H)}$ as described in Preparation of Hydrated Stratum Corneum (dry weight 6.95–25.45 mg per piece). A SC sheet was immersed in 2 ml LVP containing 32.20–92.15 µg/ml$^{(d,h)}$, 57.93–75.49 µg/ml$^{(NaCl)}$, and 57.93 µg/ml$^{(H)}$ CAF; 12.12–403.37 µg/ml$^{(d)}$, 39.17–403.37 µg/ml$^{(h)}$, 12.12 µg/ml$^{(NaCl)}$ and

12.12–48.92 μg/ml$^{(H)}$ FFA; 9.60–414.45 μg/ml$^{(d,h)}$, and 9.60–188.87 μg/ml$^{(NaCl,H)}$ TST and allowed to equilibrate at 32°C for 24 h.

To exclude unspecific adsorption to the test tubes these were incubated with the drug solution alone. Furthermore, to exclude that substances interfering with analytics are extracted by the solvent, a piece of SC was soaked with the vehicle for 24 h and underwent the same procedure as the drug containing solutions.

All partition coefficients are reported relative to the volume of dry SC independent of the hydration state of the SC.

Influence of Hydration

SC either freeze-dried or gradually hydrated as described in "Preparation of Hydrated Stratum Corneum" were subjected to the procedure as described in "Influence of Concentration of Incubation Solution". A minimum of four repetitions was performed for each hydration state. Afterwards samples were drawn from the LVP and analyzed for drug contents via UV spectroscopy.

Quantification of Caffeine, Flufenamic Acid, and Testosterone

Extraction of Testosterone from Low Viscous Paraffin

The extraction method substitutes the UV quantification below the lower limit of quantification. The equilibration experiment was performed as described above. After establishing equilibrium 1 ml of the donor were transferred into a glass test tube and 2 ml of methanol were added. The mixture was vortexed intensely and the non-miscible phases were allowed to separate at room temperature. A sample was drawn from the upper phase (methanol) and analyzed by HPLC/UV-Vis. If necessary, samples were diluted prior to the analysis. In preliminary experiments the extraction efficiency in the concentration range of 10–200 μg/ml had been found to be 95±5%.

The extraction was performed at c_{don} 9.6, 24.1, and 188.87 μg/ml using $n=5$ for each concentration and each hydration method as well as "dry" SC resulting in overall 60 samples. The samples at 188.87 μg/ml serve as a control that the results of the extraction method are not different from the UV measurement and therefore can be combined. A t-test comparing results from extraction experiments at 188.87 μg/ml with all results from UV measurements above 50 μg/ml found no statistical differences on the 95% confidence level.

UV-spectroscopy

Samples dissolved in LVP were analyzed by UV-spectroscopy at 270, 284, and 250 nm (CAF, FFA, and TST, respectively) after adding dichloromethane (DCM) up to a final ratio of LVP/DCM of 1:10. For all compounds a calibration was performed using external standards containing 3.75–20 μg/ml CAF (limit of quantification LOQ: 3 μg/ml), 3.125–15 μg/ml FFA (LOQ: 1 μg/ml), or 5–15 μg/ml TST (LOQ: 5 μg/ml) dissolved in the same medium as the unknown samples, *i.e.* 10% *V/V* LVP/DCM. If necessary, unknown samples were diluted to an appropriate concentration with 10% *V/V* LVP/DCM. UV cuvettes were sealed with parafilm and aluminium foil to prevent evaporation of the volatile DCM.

HPLC

Samples dissolved in (Soer,7.4) or methanol were analyzed by RP-HPLC using an isocratic Dionex HPLC system (Lichrospher® RP-18 column/ 125×4 mm/ 5 μm with a LiChroCART® 4–4 guard column (Merck-Hitachi, Darmstadt); Software: chromeleon 6.50 SP2 build 9.68.

CAF. Mobile phase: 90:10 (*V/V*) buffer pH 2.6/acetonitrile; retention time: 5.1±0.2 min; flow rate: 1.2 ml/min; injection volume: 50 μl; detection wavelength: 270 nm; detection limit: 10 ng/ml; quantification limit: 50 ng/ml

FFA. Mobile phase: 80:20 (*V/V*), methanol/ buffer pH 2.2; retention time: 3.5±0.2 min; flow rate: 1.2 ml/min; injection volume: 50 μl; detection wavelength: 284 nm; detection limit: 15 ng/ml; quantification limit: 50 ng/ml

TST. Mobile phase: 70:30 methanol/ water (*V/V*); retention time: 4.8 min±0.2 min; flow rate: 1.2 ml/min; injection volume: 50 μl; detection wavelength: 250 nm; detection limit: 15 ng/ml; quantification limit: 50 ng/ml

For all compounds a calibration was performed using external standards with 0.05–25 μg/ml dissolved in the same medium as the unknown samples, *i.e.* Soerensen buffer pH 7.4 or methanol. If necessary, unknown samples were diluted to an appropriate concentration with the same medium prior to analysis.

Software

All calculations were performed with Origin 7.5G SR3, OriginLab Corporation, Northampton, MA, USA.

RESULTS

Hydration

The aim was to span a wide range of hydration states. This could be realised by hydrating SC sheets above or within salt solutions or pure water. Different salt solutions or a saturated atmosphere have repeatedly been used for hydrating skin. Commonly, sodium bromide 27% *w/w* (10), saturated sodium carbonate (10), potassium carbonate 5.7–1.4 M (73,74), and saturated barium chloride (75) are used to generate specific relative humidities in a vapor sealed environment. The mole fraction of a sodium bromide 27% *w/w* solution is equivalent to a sodium chloride 15.32% *w/w* solution, *i.e.* 2.62 M.

Due to thermodynamic equilibrium SC hydration should basically be the same after equilibration above water in a saturated atmosphere and after immersion. However, there is microscopical evidence that swelling is profoundly different in humid air and after immersion, the latter resulting in significant water uptake into selective zones of the SC (76). The immersion procedure is relevant for the measurement of partition coefficient experiments with aqueous vehicles and for *in vitro* Franz-diffusion cell experiments with aqueous donor and acceptor media. In order to investigate possible influences on $K_{SC/don}$ we additionally investigated SC that had been hydrated in a saturated atmosphere. Here, no influence on the SC structure had been reported (76).

Table II. Sources and Results of Input parameters Used in M1 and M2 for CAF, FFA, and TST

	CAF	FFA	TST
$K_{lip/Soer}$	2.15±0.42 (6)	20.32±0.54 (6)	n.a.
s_{aqu} (mg/ml)	24.87±0.90	pH 6.5: 0.43±0.014 pH 5.5: 0.041±0.002	0.02±0.001
s_{LVP} (mg/ml)	0.134±3.31×10^{-3}	1.18±0.05	0.50±0.06
$K_{lip/LVP}$	399.03	35.40	15.67
$K_{aqu/LVP}$	185.6	pH 6.5: 0.36 pH 5.5: 0.035	0.047
$q_{max,ker}$ (µg/mg)	n.a.	77.03±7.08 (6)	2.16±1.36
k_{ker} (ml/µg)	n.a.	1.28×10^{-3}±2.4×10^{-4} (6)	0.0517±0.045

n.a. not available

Equilibration of SC sheets over 15.32% *w/w* sodium chloride solution, pure water or immersion in water resulted in hydration of 31 - 79% *w/w* (n=16), 46–212% *w/w* (n=83), and 445–780% *w/w* (n=25). The SC hydration is highly sensitive to small changes in the relative humidity of the environment especially during weighting. Therefore the SC water content that was reached with one hydration method varied rather largely. Furthermore these variations may be due to quantities of natural moisturizing factors varying between skins of different patients. For the evaluation of partition coefficients the accurate level of hydration of each individual SC sheet was taken into account instead of using a mean hydration level for all SC sheets hydrated with the same method.

Input Parameters

Table II gives an overview over the sources and results of the input parameters needed for the compartmental models M1 and M2 as introduced in "Theory". Data gathered from the literature are marked as such. Further data that have been determined in the course of this work are presented in detail below.

Determination of Saturation Concentration

The solubility in Soer,7.4 and LVP is as expected from the compound lipophilicity *i.e.* Soer,7.4: CAF>TST; LVP: FFA> TST>CAF (Table II). As a weak acid the aqueous solubility of FFA is pH dependent and higher at pH 6.5 than at pH 5.5.

Keratin Binding of Testosterone

TST exhibits a concentration dependent keratin binding (Fig. 2). The dependence of bound (µg/mg keratin) on free concentration (µg/ml) at equilibrium at 32°C is expressed by a Langmuir adsorption isotherm (Eq. 9). The Langmuir adsorption constant k_{ker} and the maximum loading capacity $q_{max,ker}$ were determined by non-linear regression (Table II; χ^2= 0.00879; r^2=0.888). However, due to the low aqueous solubility of TST the predicted $q_{max,ker}$ cannot be confirmed experimentally. The uncertainty of $q_{max,ker}$ is irrelevant in the models as by definition the maximum free concentration available for keratin binding equals the aqueous solubility of TST (compare "Definition of Compartments and Interfaces"). At low ratios of compound to protein the linear part of the isotherm applies.

Mechanism of Corneocyte Interaction—Experimental Results

Experimentally, two ways of substance-corneocyte interactions can be identified at least qualitatively. These are an involvement of SC water and binding to proteins. As described, a non-aqueous donor allows working with SC at defined water content so that the role of hydration on the SC-donor partition coefficient can be investigated. Figure 3A shows that only $K_{SC,dry/don}$ of the highly water soluble CAF depends on $\omega^{aqu}_{SC,dry}$. For the lipophilic poorly water soluble compounds FFA and TST the degree of membrane hydration does not influence the SC partition coefficient (Fig. 3B, C). Therefore, for the lipophilic compounds we will not distinguish between the hydration methods in the further course of this article. It is further evident that with increasing hydration $K_{SC,dry/don}$ of CAF is higher than $K_{SC,dry/don}$ of FFA and TST indicating a higher affinity to hydrated SC of CAF compared to FFA and TST.

Furthermore, a dependence of $K_{SC,dry/don}$ on c_{don} indicates an underlying saturable process such as binding to a limited number of available protein binding sites. Figure 4 shows the results for FFA and TST which were already known to bind to isolated bovine keratin in a saturable fashion. For both

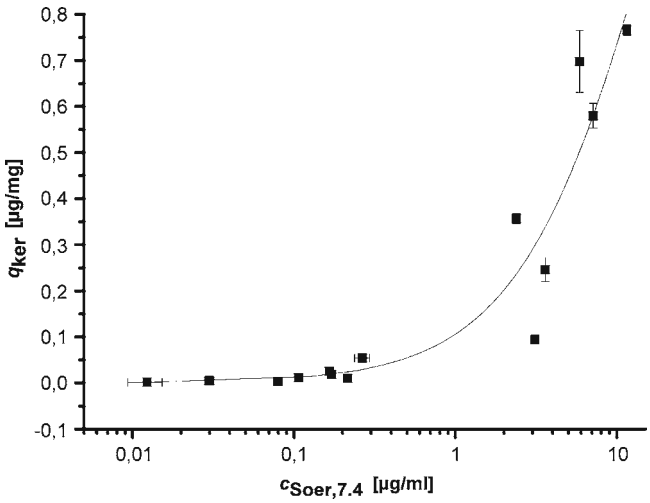

Fig. 2. The Langmuir isotherm accurately represents the concentration dependence of TST binding to keratin. (n=3 for each level of $c_{Soer,7.4;}$ standard deviation displayed as error bars; for most points the size of the error bars falls within the size of the symbols).

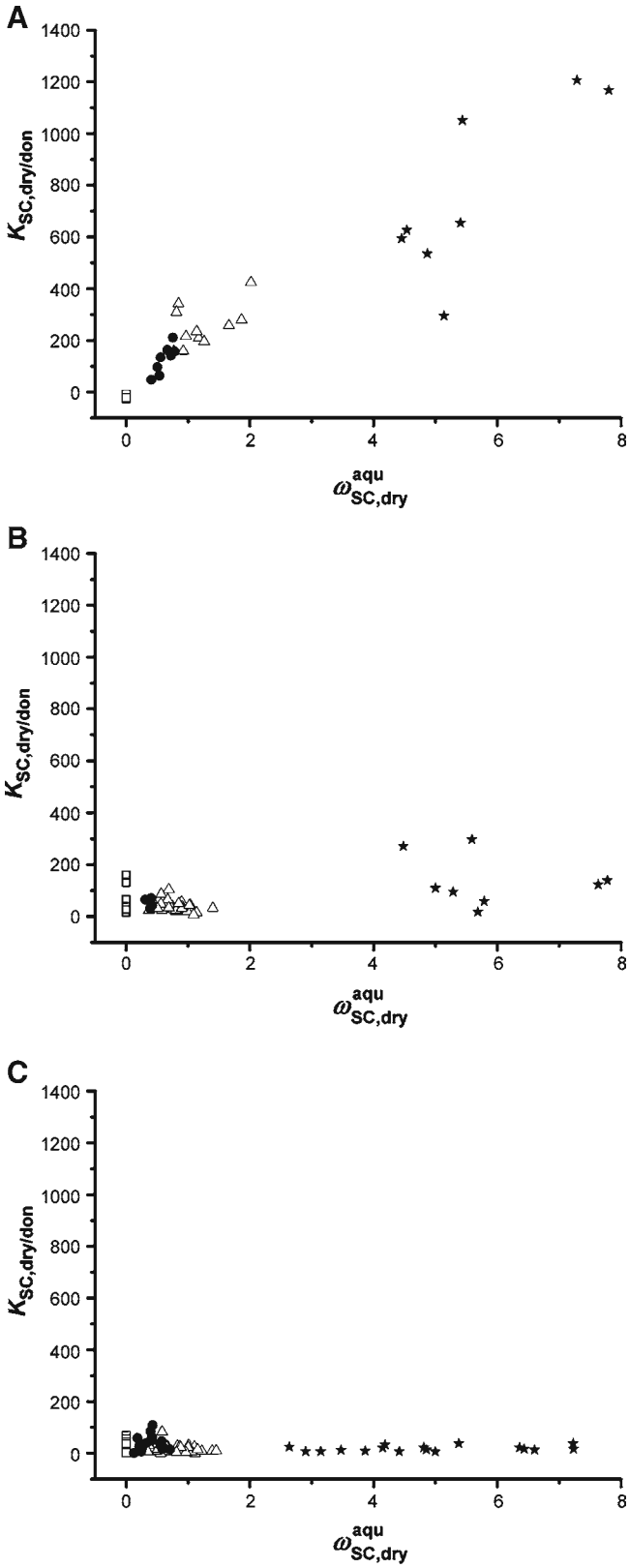

Fig. 3. Experimentally measured $K_{SC,dry/don}$ of the hydrophilic CAF (**A**) increases with progressive SC hydration. For the lipophilic compounds FFA (**B**) and TST (**C**) SC hydration has no influence on $K_{SC,dry/don}$. (*open square* dry SC, *filled circle* hydrated above NaCl, *open triangle* hydrated above water, *filled star* hydrated in water; each point is a measurement of an individual piece of SC).

compounds a concentration dependence of $K_{SC,dry/don}$ is present in the concentration range below 50–100 μg/ml. This is more pronounced for FFA than for TST. As expected $K_{SC,dry/don}$ of the non-keratin binding CAF does not depend on concentration at a defined $\omega^{aqu}_{SC,dry}$ (results not shown).

Mechanism of Corneocyte Interaction—Comparison of Theoretical and Experimental Results

Non-keratin Binding Compounds: Caffeine

Figure 5A compares experimentally determined $K_{SC,dry/don}$ measured at different SC hydration levels (open squares) with the values predicted (bold solid line) according to Eq. 18 (dry SC) and Eq. 22 and Eq. 23 (hydrated SC). Remember that for non-keratin binding substance there is no difference between M1 and M2. For the predictions the same range of $\omega^{aqu}_{SC,dry}$ was chosen

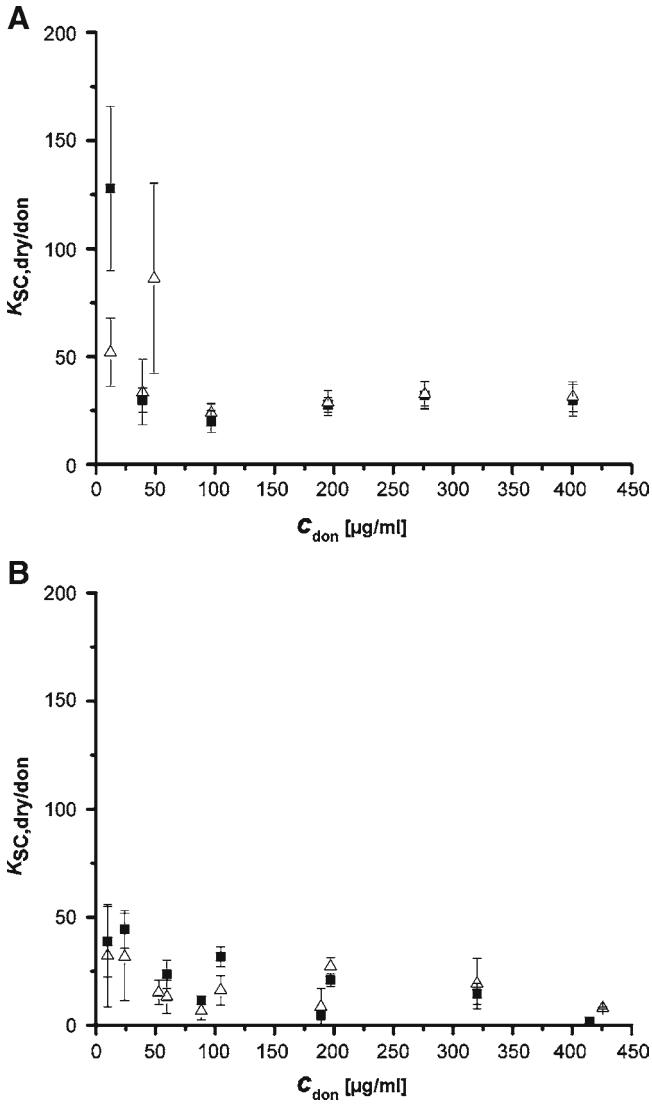

Fig. 4. $K_{SC,dry/don}$ of keratin binding substances FFA (**A**) and TST (**B**) were measured as a function of donor concentration. $K_{SC,dry/don}$ increases in the lower concentration range whereas it is relatively constant at high concentrations. The different symbols indicate the applied hydration method (*filled square* dry SC, *open triangle* hydrated SC; n=2–15; standard deviation displayed as error bars).

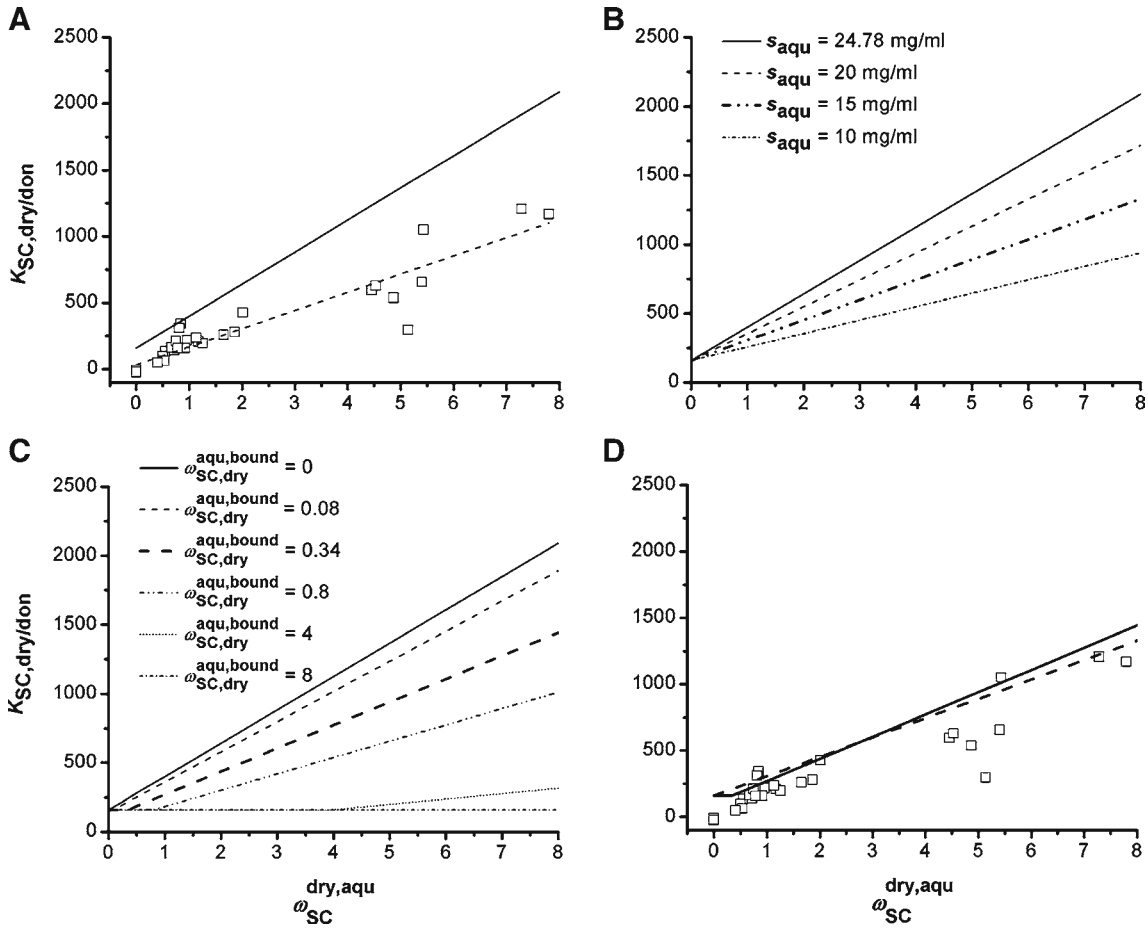

Fig. 5. Comparison of experimental and calculated $K_{SC,dry/don}$ as a function of $\omega^{aqu}_{SC,dry}$ for CAF. **A** The model overestimates the impact of hydration on $K_{SC,dry/don}$ (*open squares* experiment; *dashed line* linear fit of experimentally determined $K_{SC,dry/don}$ against $\omega^{aqu}_{SC,dry}$; *straight line* calculated $K_{SC,dry/don}$ for $0 \le \omega^{aqu}_{SC,dry} \le 8$. **B**, **C** results of the optimization strategies: **B** effect of a reduction of s_{aqu}; **C** effect of an increasing bound water fraction. **D** The experimental data is compared to optimized predictions (*open squares* experiment; *bold dashed line* s_{aqu} reduced to 15 mg/ml; *bold straight line* bound water fraction of $\omega^{aqu,bound}_{SC,dry} = 0.34$).

as in the experiment. A linear regression provides for the experimental results a slope of 137.11±9.11 and an offset of 31.45±25.99 (expressed as mean±SE; r^2=0.869). The slope signifies the increase of $K_{SC,dry/don}$ due to an uptake of 1 g water per 100 g dry SC. The offset is determined by $K_{SC,dry/don}$ at zero hydration which indicates the affinity of CAF to the lipid compartment. Due to the substantial scatter of the experimental data the estimated offset is subject to a high variation. In both experiment and prediction $K_{SC,dry/don}$ depends linearly on $\omega^{aqu}_{SC,dry}$. The compartmental model overestimates the impact of $\omega^{aqu}_{SC,dry}$ on $K_{SC,dry/don}$ and suggests a steeper slope than seen *in vitro* as well as a higher offset. Predicted values for slope and offset are 241.28 and 159.94 (compare to "Mechanism of Corneocyte Interaction—Experimental Results").

For CAF it could be shown earlier that it does not bind to keratin. Therefore no concentration dependence of $K_{SC,dry/don}$ was expected. Nonetheless, to confirm the theory a range of concentrations was tested. Any influence of concentration on partitioning should have produced a deviance from the theory. This was not the case as shown *e.g.* in Fig. 5.

Two possible influencing factors were investigated on a theoretical level in order to evaluate their potential to influence the affinity of CAF to the aqueous compartment. This is first s_{aqu} that directly enters $K_{aqu/don}$ (see "the Aqueous Compartment–Low Viscous Paraffin Partition Coefficient $K_{aqu/LVP}$"). The influence of a systematic decrease of s_{aqu} on $K_{SC,dry/don}$ at increasing $\omega^{aqu}_{SC,dry}$ in steps of 5 mg/ml starting with $s_{Soer\ 7.4}$ is shown in Fig. 5B. As s_{aqu} is reduced a progressive hydration leads to a more shallow increase of $K_{SC,dry/don}$ with $\omega^{aqu}_{SC,dry}$ with s_{aqu} best mimicking the experimental slope.

As a second influencing factor the volume fraction of the aqueous phase available for compound uptake was investigated. So far we considered the whole aqueous phase accessible for compound dissolution although it is well known that substantial portions of water are bound to SC proteins and natural moisturizing factors. It has long been recognized for liposomes that water that is bound strongly to lecithin is not accessible for compound partitioning (60). This concept has also been adopted for hydration of SC keratin (77). Hadgraft *et al.* as well as others determined a portion of $\omega^{aqu,bound}_{SC,dry} = 0.34$ as bound water ($\omega^{aqu,bound}_{SC,dry}$ being the weight of bound water per weight of dry SC) which would consequently be unavailable for partitioning. Any additional water is considered free water with dissolution properties exactly as bulk water. A bound water fraction can easily be implemented into the model. $\omega^{aqu,bound}_{SC,dry}$ is transferred

to $\varphi_{SC,hyd}^{aqu,bound}$ as described in "Appendix A" which is than subtracted from $\varphi_{SC,hyd}^{aqu}$:

$$K_{SC,dry/don} = \frac{\varphi_{SC,hyd}^{lip} K_{lip/don} + \left(\left|\varphi_{SC,hyd}^{aqu} - \varphi_{SC,hyd}^{aqu,bound}\right|\right) K_{aqu/don}}{\varphi_{SC,hyd}^{SC,dry}} \quad (31)$$

To illustrate the dependence of $K_{SC,dry/don}$ on $\omega_{SC,dry}^{aqu,bound}$ the level of $\varphi_{SC,hyd}^{aqu,bound}$ was varied (Fig. 5C). For $\varphi_{SC,dry}^{aqu} \leq \varphi_{SC,dry}^{aqu,bound}$ the modulus in Eq. 31 is zero so that the term describing the affinity to the aqueous compartment is deleted. In other words if the number of water molecules within the SC is smaller than the number of water binding sites then all water will be bound and none will be available for compound dissolution. $K_{SC,dry/don}$ will now exclusively be determined by uptake into the SC lipids and $K_{SC,dry/don}$ against $\omega_{SC,dry}^{aqu}$ gives a straight line parallel to the *x*-axis (Fig. 5C). For $\varphi_{SC,dry}^{aqu} > \varphi_{SC,dry}^{aqu,bound}$ any additional water will again be available for compound dissolution and $K_{SC,dry/don}$ increases linearly with $\omega_{SC,dry}^{aqu}$ (Fig. 5C). However, the slope will depend on the height of $\omega_{SC,dry}^{aqu,bound}$. $\omega_{SC,dry}^{aqu,bound} = 0.34$ is indicated by a bold dotted line. Figure 5D compares the estimate for $\omega_{SC,dry}^{aqu,bound} = 0.34$ (bold dotted line) and s_{aqu}=15 mg/ml with the experimental data (open squares). Both correction strategies offer an equally good representation of the slope of the experimental data. The problem of overemphasising the offset of the experimental curve is not solved by either correction strategy.

Keratin Binding Compounds: Flufenamic Acid and Testosterone

Figure 6 compares predictions of M1 for varying degrees of SC hydration in the range of $\omega_{SC,dry}^{aqu} = 0 - 8$ (Eqs. 18 and 19) with experimental results on the dependency of $K_{SC,dry/don}$ on c_{don}. Experimental data are shown as means and standard deviation for dry (open squares) and hydrated SC (open triangles). Results predicted with M1 are shown as lines (bold dashed line: $\omega_{SC,dry}^{aqu} = 0$). Figure 6A gives the results for FFA. Here, additionally, two different values for pH_{aqu} were considered in the theoretical analysis. In M1 according to Eq. 18 $K_{SC,dry/don}$ for dry SC is exclusively influenced by the compound affinity to the lipid compartment. As the lipid concentration c_{lip} is described via a simple proportionality (Eq. 8) M1 predicts $K_{SC,dry/don}$ of dry SC to be independent of c_{don}. M1 implicates a donor concentration dependence only for hydrated SC which is accounted for by a Langmuir isotherm (Eq. 9**)**. Considering a pH_{aqu} of 5.5 (which was approximately the lower margin of pH-values investigated in SC (67)) the solubility of FFA in the aqueous compartment is very low (Table II). This leads to a very low $K_{aqu/don}$ which enters Eq. 19 in the term describing the compound affinity to the aqueous phase and the Langmuir isotherm quantifying protein binding. Therefore at pH_{aqu} 5.5 M1 predicts $K_{SC,dry/don}$ to be practically independent of SC hydration and independent of donor concentration. At pH_{aqu} 6.5, which would be approximately the upper margin of pH values investigated in human SC (67), $K_{aqu/don}$ is an order of magnitude higher than at pH_{aqu} 5.5. The effect on $K_{SC,dry/don}$ is however still limited. Compared to dry SC M1 predicts that hydration of the SC provokes a four to five times elevated $K_{SC,dry/don}$. Finally, the absolute level of hydration is rather unimportant such as in the range of

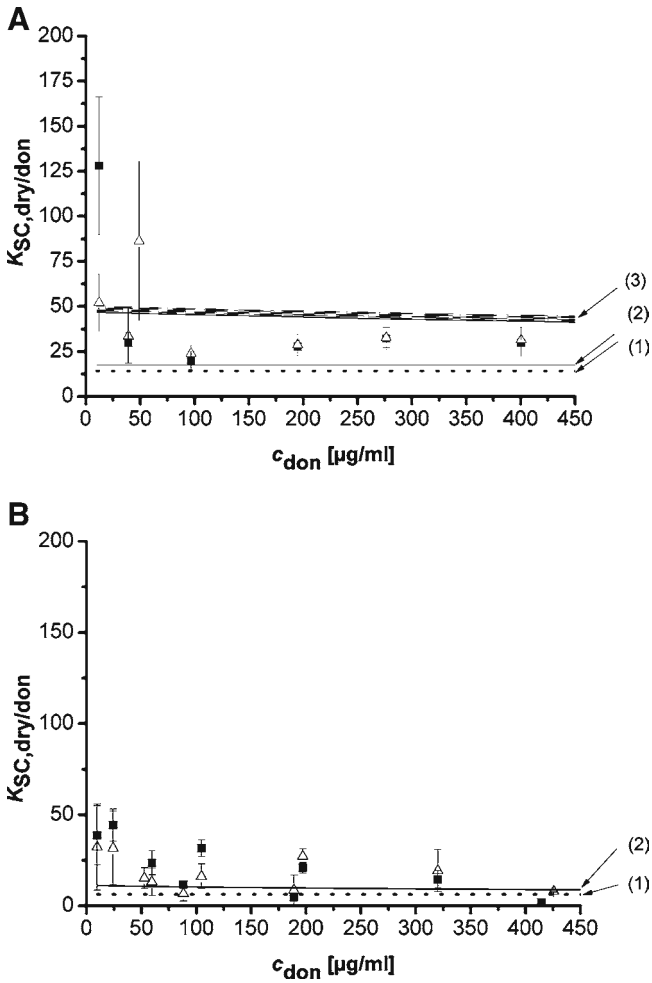

Fig. 6. M1: Comparison of experimental and calculated $K_{SC,dry/don}$ as a function of c_{don} for varying $\omega_{SC,dry}^{aqu}$ for **A** FFA and **B** TST (experimental results: dry SC (*filled square*); SC hydrated (*open triangle*)). Calculated results, **A**: (*1*) $\omega_{SC,dry}^{aqu} = 0$; (*2*) pH_{aqu}=5.5; $0 < \omega_{SC,dry}^{aqu} \leq 8$; (*3*) pH_{aqu}=6.5; $0 < \omega_{SC,dry}^{aqu} \leq 8$; **B**: (*1*) $\omega_{SC,dry}^{aqu} = 0$; (*2*) $0 < \omega_{SC,dry}^{aqu} \leq 8$). For FFA the influence of the pH_{aqu} was investigated using the upper and lower margin determined by a tape-stripping method with surface parallel pH electrodes (67).

$0 < \omega_{SC,dry}^{aqu} \leq 8$ an increasing $\omega_{SC,dry}^{aqu}$ influences $K_{SC,dry/don}$ negligibly (Fig. 6A). The range of $K_{SC,dry/don}$ predicted by M1 within the pH_{aqu} range of 5.5 and 6.5 includes the major portion of the experimental values. At pH_{aqu} 5.5 M1 further correctly predicts the independency of hydration. However, obviously in both cases M1 is not able to correctly express the concentration dependence of $K_{SC,dry/don}$ at low c_{don} that was seen in the experiment.

Figure 6B shows the results for TST. Experimental partition coefficients were in the range of 1.81±0.24 to 50.13±22.53. In the concentration range below 50 µg/ml $K_{SC,dry/don}$ increases with decreasing c_{don}. In contrast M1 predicts $K_{SC,dry/don}$ of 6.28 for dry SC and 8.47 to 11.42 for hydrated SC, both being independent of $\omega_{SC,dry}^{aqu}$ as well as c_{don}. Due to the similar $K_{aqu/don}$ of FFA at pH_{aqu} 5.5 and TST the influence of hydration on $K_{SC,dry/don}$ is similarly negligible as for FFA.

The predictions of M2 (Eq. 20 and Eq. 21) are shown in Fig. 7 (left hand-side FFA, right hand-side TST). Figure 7A1

and B1 were calculated assuming $k_{cpe}=10^{-3}$ ml/µg which would be considered as a kind of lower margin where the compound affinity to the cpe is very limited. This is combined with different levels of maximum binding capacity $q_{max,cpe}$ of 1, 10, 50, and 100 µg/mg, *i.e.* from a rather moderate to a substantial maximum binding capacity. Furthermore the influence of the aqueous compartment was considered by predicting $K_{SC,dry/don}$ for the lower and upper limit of SC hydration *i.e.* $\omega^{aqu}_{SC,dry}=0$ (bold lines) and $\omega^{aqu}_{SC,dry}=8$ (thin lines). (A1 and B1) At $k_{cpe}=10^{-3}$ ml/µg a $q_{max,cpe}=1$ µg/mg is not sufficient to provoke a concentration dependence of $K_{SC,dry/don}$. With increasing $q_{max,cpe}$ two effects are obvious: (1) the concentration dependence at low c_{don} becomes more pronounced, *i.e.* the slope of $K_{SC,dry/don}$ against c_{don} becomes steeper, (2) $K_{SC,dry/don}$ in the whole concentration range is increased, with the increase being more pronounced at lower c_{don}. An increase in $q_{max,cpe}$ however does not lead to an increased influence of $\omega^{aqu}_{SC,dry}$ on $K_{SC,dry/don}$. These trends are evident both in the predictions for FFA and TST. For TST at identical combinations of k_{cpe} and $q_{max,cpe}$ the slope of the curve at low c_{don}, *i.e.* in the range where the cpe shows its influence, is slightly less steep than with FFA.

Figure 7A2 and B2 were calculated assuming $k_{cpe}=10^{3}$ ml/µg, *i.e.* an upper margin marking a high compound affinity to the cpe. This is again combined with different levels of $q_{max,cpe}$ of 1, 10, 50, and 100 µg/mg. Again the influence of the aqueous compartment was considered by calculating the results for the lower and upper limit of SC hydration $\omega^{aqu}_{SC,dry}=0$ (bold lines) and $\omega^{aqu}_{SC,dry}=8$ (thin lines). Now, already even for $q_{max,cpe}=1$ mg/mg there is a (however limited) non-linear concentration influence on $K_{SC,dry/don}$. In general, compared to the estimates with $k_{cpe}=10^{-3}$ ml/µg (1) the absolute height of the predicted $K_{SC,dry/don}$ is higher, especially in the lower range of c_{don}, (2) the slope of $K_{SC,dry/don}$ against c_{don} is steeper (the first partially being a consequence of the second).

In Fig. 8A1 and B1 the experimental results are shown together with that combination of $q_{max,cpe}$ and k_{cpe} that achieves the best prediction according to M2 (again A marks the results for FFA while B will be TST). These are for both FFA at pH_{aqu} 5.5 and TST: $q_{max,cpe}=10$ µg/mg and $k_{cpe}=10^{3}$ ml/µg. There will probably be further suitable combinations of $q_{max,cpe}$ and k_{cpe} being able to correctly express the experimental results. Therefore it was tested whether the binding parameters measured with bovine keratin could serve to give a first estimate of the binding properties of the cpe (Fig. 8A2 and B2). For FFA these estimates express the experimental results at low c_{don} less correctly than the "optimized" set of $q_{max,cpe}$ and k_{cpe}. However, the overall trend of the experimental values is expressed in the simulation. For TST the estimate using $q_{max,ker}$ and k_{ker} for describing the

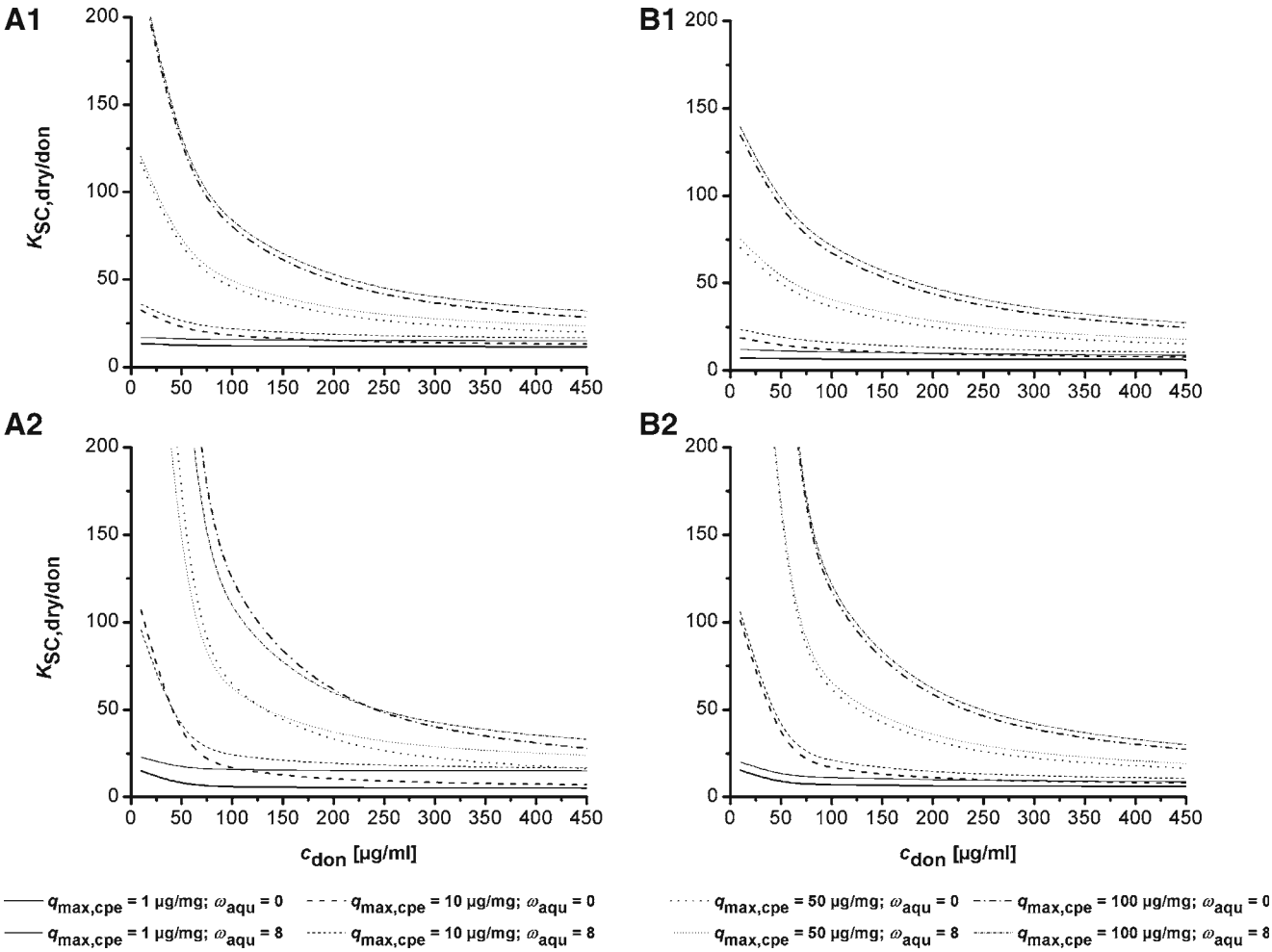

Fig. 7. M2; systematic variation of cpe maximum binding capacity $q_{max,cpe}$ (1, 10, 50, and 100 µg/mg) and cpe binding constant k_{cpe} **A** FFA; **B** TST. *A1+B1* $k_{cpe}=10^{-3}$ ml/µg. *A2+B2* $k_{cpe}=10^{3}$ ml/µg (*bold lines*: $\omega^{aqu}_{SC,dry}=0$; *thin lines*: $\omega^{aqu}_{SC,dry}=8$).

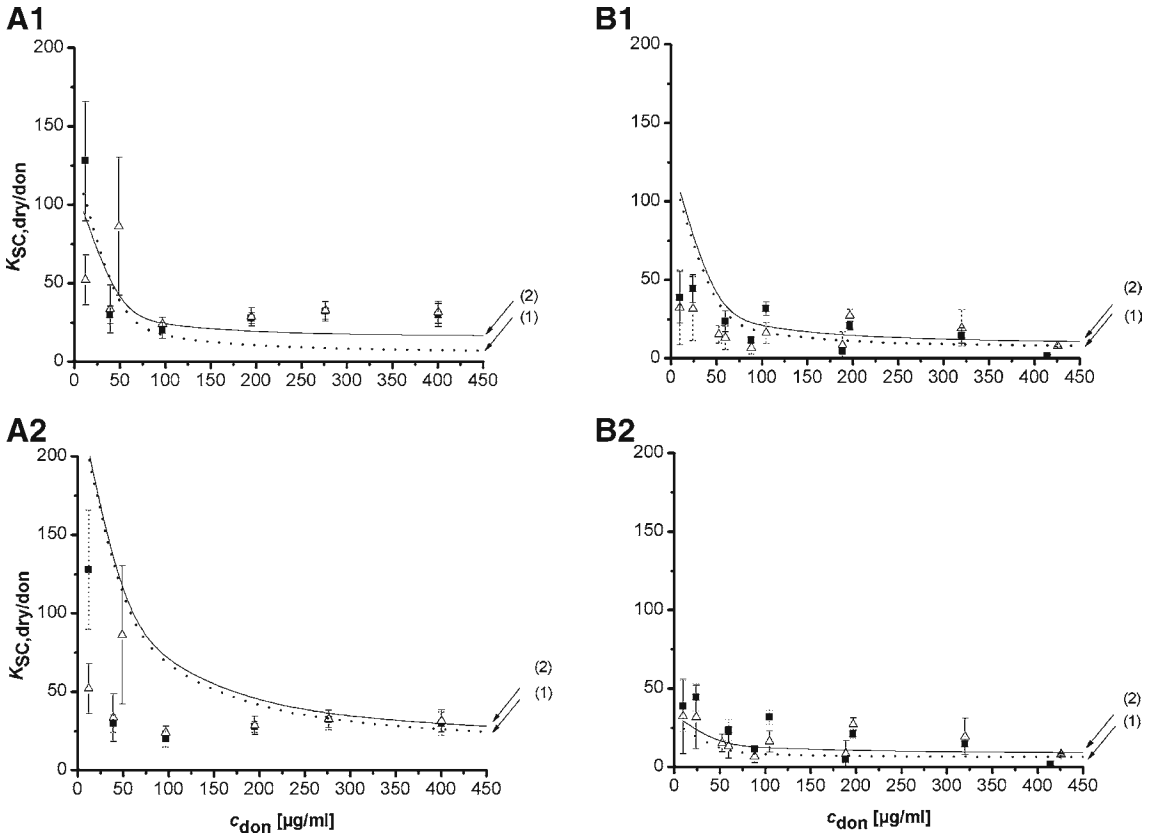

Fig. 8. M2; comparison of experimental results of FFA and TST with optimized binding parameters for cpe (*A1*: FFA: $q_{max,cpe}$=10 µg/mg, k_{cpe}=10^3 ml/µg, pH_{aqu}=5.5; *B1*: TST: $q_{max,cpe}$=10 µg/mg, k_{cpe}=10^3 ml/µg). Assuming the binding properties of the cpe to be identical to ker, *i.e.* $q_{max,cpe}=q_{max,ker}$ and $k_{cpe}=k_{ker}$ was a good first estimate of $K_{SC,dry/don}$ (*A2*: FFA, *B2*: TST) (experimental results: dry SC (*filled square*); SC hydrated (*open triangle*)). Calculated results: (*1*) $\omega^{aqu}_{SC,dry}=0$; (*2*) $\omega^{aqu}_{SC,dry}=8$).

binding properties of the cpe expresses the experimental data better than the "optimized" set of $q_{max,cpe}$ and k_{cpe}.

In summary, M2 however, not M1 is able to predict the concentration dependence of $K_{SC,dry/don}$ that is seen in the experiment. It shall be noted that the predicted influence of hydration on $K_{SC,dry/don}$ for protein binding permeants with limited water solubility is profoundly different from hydrophilic compounds. For protein binding compounds hydration acts in a two-state fashion: there is a visible difference in $K_{SC,dry/don}$ at zero hydration $\left(\omega^{aqu}_{SC,dry}=0\right)$ compared to any other hydration state $\left(\omega^{aqu}_{SC,dry}>0\right)$. However, there is practically no differentiation according to the actual water weight fraction at $\omega^{aqu}_{SC,dry}>0$. This is equally predicted by model M1 and M2 for both FFA and TST and is depicted *e.g.* in Figs. 6, 7 and 8. This is also in line with Fig. 3B and C which shows that the hydration method does not influence $K_{SC,dry/don}$ of FFA and TST.

DISCUSSION

The theoretical analysis offers a very simple method to predict the influence of the SC water content on SC partitioning. In addition, the presented experimental setup allows an easy investigation of the effect of hydration on $K_{SC,dry/LVP}$. In contrast, the Franz cell, an experimental setup that is often used in *in vitro* skin permeability measurements, is not suited for addressing this kind of question as the skin membrane will always be fully hydrated through the aqueous acceptor medium.

As a first approach to describe the interactions of CAF with the aqueous domain quantitatively the solubility in the aqueous SC compartment was assumed to be comparable to physiological buffer. However, this led to an overestimation of the impact of hydration on $K_{SC,dry/don}$. Two strategies were followed in order to reduce the affinity of CAF to the aqueous compartment. Both the reduction of the aqueous solubility and the introduction of a non-accessible water fraction could successfully reduce the slope of $K_{SC,dry/don}$ with $\omega^{aqu}_{SC,dry}$. The aqueous solubility of CAF depends on temperature, and may be increased by the presence of organic acids or their alkali salts, *e.g.* benzoates, salicylates, or citrates, while no such effect is reported for phosphate ions contained in the Soerensen buffer (78). Although Kasting *et al.* advocated for a shallow transition from bound to free water state which could result in a likewise shallow transition of solubility a two-state analysis was sufficient to reduce the dependence of $K_{SC,dry/don}$ on $\omega^{aqu}_{SC,dry}$ to values as found *in vitro* (9,69). The picture may be significantly complicated if the binding sites of water and drug compounds are identical. Then the magnitude of the binding constant would determine whether the drug is able to displace water from its binding site. However, both strategies fail to reduce the overestimated offset of the predicted $K_{SC,dry/don}$ at $\omega^{aqu}_{SC,dry}=0$ as this is only influenced by the compound affinity to the lipid compartment Eq. 18. According to "The Stratum Corneum Lipid–Low

Viscous Paraffin Partition Coefficient $K_{lip/LVP}$" this was calculated from $K_{lip/Soer,7.4}$, $s_{Soer,7.4}$, and s_{LVP}. Prerequisite for Eq. 26 is that all interacting phases are non-miscible. It is known that at high hydration levels water intercalates into SC lipids. The improved hydrophilicity of the lipid bilayer could promote the lipid affinity of hydrophilic compounds such as CAF such that the experimental value for *K*lip/Soer,7.4 is slightly overestimated. Equally, a penetration of LVP into SC lipids should lower the affinity of CAF to the SC lipids as the solubility of CAF in LVP is significantly lower than in SC lipids ($K_{lip/LVP}$ of CAF is highly positive). Both mechanisms could account for an overestimation of $K_{lip/LVP}$ of CAF and thus of $K_{SC,dry/don}$ at $\omega_{SC,dry}^{aqu} = 0$.

For a number of compounds adsorption to isolated keratin powder was reported (39,40,54,55). The question is whether keratin binding is possible in the morphological context of the membrane. Due to the unique morphology of the human SC a direct contact between keratin and intercellular lipids is highly unlikely (53). Therefore in M1 the possibility of lipid–protein interactions was ruled out completely. Instead it was assumed that compound keratin interactions will be mediated via intra-corneocyte water which in turn communicates with intercellular lipids. However, potentially protein binding compounds usually are lipophilic and therefore poorly water soluble. This was tested with the two keratin binding compounds FFA and TST that differ in their maximum binding capacity and keratin affinity constant. Varying pH_{aqu} predictions of M1 effectively showed that if there are substantial FFA concentrations within the corneocyte water $K_{SC,dry/don}$ will not so much be concentration dependent but sensitive to SC hydration. It is therefore highly unlikely that FFA enters intra-corneocyte water to a significant extent. It remains to be analysed whether the weakly acidic corneocyte pH could facilitate the corneocyte solubility of bases and thus mediate keratin access of lipophilic bases. This could provide the explanation for the significant concentration dependence of $K_{SC,dry/don}$ of scopolamine (47) although this may also have been a consequence of binding to the cpe.

Summing up these findings, the concentration dependence of $K_{SC,dry/don}$ seen in the experiment is much more likely to be a consequence of protein access directly via the lipids and not via the detour of the aqueous corneocyte phase. This can only reasonably be assumed for structures as the cpe and corneodesmosomes although we did not consider the corneodesmosomes explicitly in our analysis. Compared to the major SC component keratin such structures encompass only a very small fraction of the whole SC (30). Therefore the main question addressed with M2 was whether this might be enough to account for the measured effects. Our theoretical parameter study systematically varying the binding parameters to the cpe could show that this is indeed possible if not likely. As this approach is not feasible for applying the model to a larger database $q_{max,ker}$ and k_{ker} could be used as estimates for $q_{max,cpe}$ and k_{cpe}. This relies of course on the assumption that the binding properties of the cpe can be expressed by keratin at all, as keratin is only one of several proteins forming the cpe. In case of TST the uncertainty of $q_{max,ker}$ (compare "Keratin Binding Compounds: Flufenamic Acid and Testosterone") becomes relevant. By definition the maximum free concentration available for binding to the cpe equals c_{lip}. The lipid solubility of TST is sufficiently high that the non-linear part of the isotherm is reached. For FFA $q_{max,ker}$ was estimated with higher certainty as due to a higher aqueous solubility roughly 70% saturation of binding sites were achieved (48).

The great importance of considering corneocyte interactions of not only water soluble but also lipophilic, protein binding molecules shall be explained consulting Vieth and Sladek (79) who provided a kinetic interpretation of the dual sorption theory. They assumed that the kinetics of immobilization are very rapid compared to the diffusion rate of the mobile component so that the diffusion is rate controlling and a local equilibrium between mobile and immobilized species is always maintained throughout the medium. Only the mobile species will be able to participate in the concentration gradient and thus in the diffusion process while the adsorbed species is completely immobilized and does not participate in the diffusive flux. This leads to significant differences in the effective and true diffusion coefficient and a retardation of adsorption equilibrium as some compound is removed from the pool of diffusing species. Naegel *et al.* recently noticed that the corneocyte diffusivity D_{cor} of FFA is overestimated when the interaction with the corneocyte phase is described solely via a partition coefficient (23). The magnitude of the affinity constant k, representing the ratio of the rate constant of adsorption and desorption and thus being an indicator of the binding strength, will influence the extent to which the effective diffusion coefficient will be reduced compared to a pure partitioning process. Furthermore, a large German multicentre-study aiming at a validation of reconstructed human epidermis models failed irrespective of the skin model investigated to predict experimental apparent permeability coefficient of a set of test compounds by established QSPR (quantitative structure activity relationship)-analyses that base only on molecular weight and lipophilicity parameters such as those mentioned above, or open-source software such as DermWin and Skinperm (80). It may be speculated that predictions may be improved when taking into account protein binding and hydration effects with the help of the theoretical analysis or the proposed experimental procedure.

After the present experimental findings there can be no doubt that hydration plays a central role in SC partitioning of water soluble molecules. Obviously CAF has a higher SC affinity than FFA and TST. At first sight this is contradictory to predictions that foot on a positive correlation between $\log K_{Oct/w}$ and the apparent permeability coefficient (66,81,82). This means that a hydrophilic compound such as CAF permeates the skin poorly due to a low affinity to the highly lipophilic character of the SC. This is evidently true for aqueous donor media. In addition the cited QSPRs rely on a lipid permeation pathway that excludes the trans-cellular route.

CONCLUSION

Equilibration experiments with gradually hydrated SC using a non-aqueous donor medium are an efficient method to investigate the impact of water uptake into the SC on SC partitioning of compounds. Together with keratin binding studies they offer experimental tools to investigate the mechanism of corneocyte interactions of compounds partitioning into the SC. The corneocytes are a distribution compartment for both lipophilic and hydrophilic compounds.

Hydrophilic water soluble molecules will predominantly interact with water that is present within healthy SC *in vivo* or additional water that has entered the corneocytes through hydration in the course of occlusive conditions. For lipophilic compounds the aqueous compartment does not play a role in SC partitioning. Although these compounds could be shown to bind to isolated keratin this is probably meaningless for the SC-donor partition coefficient. Due to their low aqueous solubility only a very limited number of molecules will find access to intra-corneocyte proteins. Thus keratin binding is limited by the aqueous solubility of a compound. An involvement of extra-cellular proteins might be of much more importance for SC uptake of lipophilic protein binding molecules.

ACKNOWLEDGEMENTS

The DFG (Deutsche Forschungsgemeinschaft; DFG Grant BIZ 4/1), the ZEBET (Zentralstelle zur Erfassung und Bewertung von Ersatz- und Ergänzungsmethoden zum Tierversuch) are thanked for financial support. Parts of this work have been performed in the course of a diploma thesis financed by the Erasmus/Sokrates program. Miss Lenka Kolackova is thanked for establishing UV-analytics.

APPENDIX A: THE VOLUME FRACTIONS OF THE SC COMPARTMENTS

Conventionally water, lipid or protein content within SC is expressed as weight fractions relative to the weight of dry SC, for example

$$\omega^{\text{lip}}_{\text{SC,dry}} = \frac{w_{\text{lip}}}{w_{\text{SC,dry}}} \tag{32}$$

For convenience and easy comparison with other authors we also use weight fractions for representation of data. However, for calculations we need volume fractions relative to the volume of dry as well as hydrated SC. This section will explain how weight and volume fractions are related. The derivation of $\varphi^{i}_{\text{SC,hyd}}$ from $\omega^{i}_{\text{SC,dry}}$ will be shown here exemplarily for $\varphi^{\text{lip}}_{\text{SC,hyd}}$ for M1 but can be done analogously for all other compartments as well as for M2. We assume dry SC to be composed of 30% *w/w* lipids, *i.e.* $\omega^{\text{lip}}_{\text{SC,dry}} = 0.3$ and 70% *w/w* proteins $\omega^{\text{pro}}_{\text{SC,dry}} = \omega^{\text{SC,dry}}_{\text{SC,dry}} - \omega^{\text{lip}}_{\text{SC,dry}} = 1 - \omega^{\text{lip}}_{\text{SC,dry}} = 0.7$. These are empirical values recorded in our lab *in vitro* for female abdominal skin of 14 different patients in 136 samples by lipid extraction of freeze-dried SC and weighing. $\omega^{\text{cpe}}_{\text{SC,dry}}$ was previously determined to be 0.07 (30) so that $\omega^{\text{ker}}_{\text{SC,dry}} = \omega^{\text{pro}}_{\text{SC,dry}} - \omega^{\text{cpe}}_{\text{SC,dry}} = 0.63$. Due to the definition in Eq. 2 we obtain

$$\omega^{\text{lip}}_{\text{SC,hyd}} = \frac{w_{\text{lip}}}{w_{\text{SC,dry}} + w_{\text{aqu}}} \tag{33}$$

where the last identity results from dividing both numerator and denominator by $w_{\text{SC,dry}}$

$$\omega^{\text{lip}}_{\text{SC,hyd}} = \frac{\frac{w_{\text{lip}}}{w_{\text{SC,dry}}}}{\frac{w_{\text{SC,dry}}}{w_{\text{SC,dry}}} + \frac{w_{\text{aqu}}}{w_{\text{SC,dry}}}} = \frac{\omega^{\text{lip}}_{\text{SC,dry}}}{1 + \omega^{\text{aqu}}_{\text{SC,dry}}} \tag{34}$$

Therefore $\omega^{i}_{SC,hyd}$ varies depending on the extent of SC hydration $\omega^{aqu}_{SC,hyd}$ in contrast to $\omega^{i}_{SC,dry}$ which is always constant. Relating Eq. 34 to the specific densities the volume fractions of the respective compartments are calculated:

$$\varphi^{\text{lip}}_{\text{SC,hyd}} = \omega^{\text{lip}}_{\text{SC,hyd}} \frac{\rho_{\text{SC,hyd}}}{\rho_{\text{lip}}} \tag{35}$$

with the density of hydrated SC defined as

$$\rho_{\text{SC,hyd}} = \frac{1}{\omega^{\text{lip}}_{\text{SC,dry}}/\rho_{\text{lip}} + \omega^{\text{pro}}_{\text{SC,dry}}/\rho_{\text{pro}} + \omega^{\text{aqu}}_{\text{SC,dry}}/\rho_{\text{aqu}}} \tag{36}$$

For dry SC and SC lipids the following densities are reported in literature: $\rho_{\text{SC,dry}}$=1.3 g/cm^3, and ρ_{lip}=0.973 g/cm^3 (72,83). The density of SC proteins can be calculated from $\rho_{\text{SC,dry}}$ as shown in Eq. 37 for M1.

$$\rho_{\text{SC,dry}} = \frac{w_{\text{SC,dry}}}{V_{\text{SC,dry}}} = \frac{w_{\text{SC,dry}}}{\frac{w_{\text{lip}}}{\rho_{\text{lip}}} + \frac{w_{\text{pro}}}{\rho_{\text{pro}}}} \tag{37}$$

Dividing both numerator and denominator by $w_{\text{SC,dry}}$ Eq. 37 may be expressed in terms of weight fractions:

$$\rho_{\text{SC,dry}} = \frac{w_{\text{SC,dry}}/w_{\text{SC,dry}}}{\frac{w_{\text{lip}}/w_{\text{SC,dry}}}{\rho_{\text{lip}}} + \frac{w_{\text{pro}}/w_{\text{SC,dry}}}{\rho_{\text{pro}}}} = \frac{1}{\frac{\omega^{\text{lip}}_{\text{SC,dry}}}{\rho_{\text{lip}}} + \frac{\omega^{\text{pro}}_{\text{SC,dry}}}{\rho_{\text{pro}}}} \tag{38}$$

$$\rho_{\text{pro}} = \frac{\omega^{\text{pro}}_{\text{SC,dry}}}{\frac{1}{\rho_{\text{SC,dry}}} - \frac{\omega^{\text{lip}}_{\text{SC,dry}}}{\rho_{\text{lip}}}} \tag{39}$$

After reorganisation for ρ_{pro} the protein density was calculated as 1.52 g/cm^3. This value is well within the experimentally determined range (84). We assumed ρ_{ker} and ρ_{cpe} to be equal to ρ_{pro}.

APPENDIX B: TRANSFORMATION OF PARTITION COEFFICIENTS

According to Eq. 17 the partition coefficients $K_{\text{SC,dry/don}}$ and $K_{\text{SC,hyd/don}}$ can be written as

$$K_{\text{SC,dry/don}} = \frac{c_{\text{SC,dry}}}{c_{\text{don}}} = \frac{w/V_{\text{SC,dry}}}{w/V_{\text{don}}} \tag{40}$$

$$K_{\text{SC,hyd/don}} = \frac{c_{\text{SC,hyd}}}{c_{\text{don}}} = \frac{w/V_{\text{SC,hyd}}}{w/V_{\text{don}}} \tag{41}$$

So that $K_{\text{SC,dry/don}}$ and $K_{\text{SC,hyd/don}}$ are related via

$$K_{\text{SC,dry/don}} = K_{\text{SC,hyd/don}} \frac{V_{\text{SC,hyd}}}{V_{\text{SC,dry}}} = K_{\text{SC,hyd/don}} \frac{1}{\varphi^{\text{SC,dry}}_{\text{SC,hyd}}} \tag{42}$$

REFERENCES

1. A. C. Williams, and B. W. Barry. Penetration enhancers. *Adv. Drug Deliv. Rev.* **56**:603–618 (2004). doi:10.1016/j.addr.2003.10.025.
2. R. Panchagnula, H. Desu, A. Jain, and S. Khandavilli. Effect of lipid bilayer alteration on transdermal delivery of a high-

molecular-weight and lipophilic drug: studies with paclitaxel. *J. Pharm. Sci.* **93**:2177–2183 (2004). doi:10.1002/jps.20140.
3. A. K. Jain, N. S. Thomas, and R. Panchagnula. Transdermal drug delivery of imipramine hydrochloride. I. Effect of terpenes. *J. Control. Release*. **79**:93–101 (2002). doi:10.1016/S0168-3659(01)00524-7.
4. M. Sznitowska, S. Janicki, and A. C. Williams. Intracellular or intercellular localization of the polar pathway of penetration across stratum corneum. *J. Pharm. Sci.* **87**:1109–1114 (1998). doi:10.1021/js980018w.
5. J. Lademann, H. Richter, A. Teichmann, N. Otberg, U. Blume-Peytavi, J. Luengo, B. Weiß, U.F. Schaefer, C.-M. Lehr, R. Wepf, and W. Sterry. Nanoparticles—an efficient carrier for drug delivery into the hair follicles. *Eur. J. Pharm. Biopharm.* **66**:159–164 (2007). doi:10.1016/j.ejpb.2006.10.019.
6. N. Otberg, A. Patzelt, U. Rasulev, T. Hagemeister, M. Linscheid, R. Sinkgraven, W. Sterry, and J. Lademann. The role of hair follicles in the percutaneous absorption of caffeine. *Br. J. Clin. Pharmacol.* **65**:488–492 (2008). doi:10.1111/j.1365–2125.2007.03065.x.
7. B. W. Barry. Drug delivery routes in skin: A novel approach. *Adv. Drug Deliv. Rev.* **54**:S31–40 (2002).
8. K. D. Peck, A.-H. Ghanem, and W. I. Higuchi. Hindered diffusion of polar molecules through and effective pore radii estimates of intact and ethanol treated human epidermal membrane. *Pharm. Res.* **11**:1306–1314 (1994). doi:10.1023/A:1018998529283.
9. G. B. Kasting, and N. D. Barai. Equilibrium water sorption in human stratum corneum. *J. Pharm. Sci.* **92**:1624–1631 (2003). doi:10.1002/jps.10420.
10. J. A. Bouwstra, A. de Graaff, G. S. Gooris, J. Nijsse, J. W. Wiechers, and A. C. van Aelst. Water distribution and related morphology in human stratum corneum at different hydration levels. *J. Invest. Dermatol.* **120**:750–758 (2003). doi:10.1046/j.1523-1747.2003.12128.x.
11. U. Jacobi, T. Tassopoulos, C. Surber, and J. Lademann. Cutaneous distribution and localization of dyes affected by vehicles all with different lipophilicity. *Arch. Dermatol. Res.* **297**:303–310 (2006). doi:10.1007/s00403-005-0621-5.
12. B. Yu, K. H. Kim, P. T. So, D. Blankschtein, and R. Langer. Evaluation of fluorescent probe surface intensities as an indicator of transdermal permeant distributions using wide-area two-photon fluorescence microscopy. *J. Pharm. Sci.* **92**:2354–2365 (2003). doi:10.1002/jps.10484.
13. H. E. Boddé, I. van den Brink, H. K. Koerten, and F. H. N. de Haan. Visualization of *in vitro* percutaneous penetration of mercuric chlorite; transport through intercellular space *versus* cellular uptake through desmosomes. *J. Control. Release*. **15**:227–236 (1991). doi:10.1016/0168–3659(91)90114-S.
14. M. E. Johnson, D. A. Berk, D. Blankschtein, D. E. Golan, R. K. Jain, and R. S. Langer. Lateral diffusion of small compounds in human stratum corneum and model lipid bilayer systems. *Biophys. J.* **71**:2656–2668 (1996). doi:10.1016/S0006-3495(96)79457-2.
15. H. F. Frasch, and A. M. Barbero. Steady-state Flux and lag time in the stratum corneum lipid pathway: result from finite element models. *J. Pharm. Sci.* **92**:2196–2107 (2003). doi:10.1002/jps.10466.
16. J. A. Bouwstra, G. S. Gooris, J. A. van der Spek, and W. Bras. Structural investigations of human stratum corneum by small-angle X-ray scattering. *J. Invest. Dermatol.* **97**:1005–1012 (1991). doi:10.1111/1523-1747.ep12492217.
17. D. Kuempel, D. C. Swartzendruber, C. A. Squier, and P. W. Wertz. *In vitro* reconstitution of stratum corneum lipid lamellae. *Biochim. Biophys. Acta*. **1372**:135–140 (1998). doi:10.1016/S0005-2736(98)00053-4.
18. M. A. Lampe, A. L. Burlingame, and J. A. Whitney. Human stratum corneum lipids: characterization and regional variations. *J. Lipid Res.* **24**:120–130 (1983).
19. A. Weerheim, and M. Ponec. Determination of stratum corneum lipid profile by tape stripping in combination with high-performance thin-layer chromatography. *Arch. Dermatol. Res.* **293**:191–199 (2001). doi:10.1007/s004030100212.
20. S. Mitragotri. Modeling skin permeability to hydrophilic and hydrophobic solutes based on four permeaion pathways. *J. Control. Release*. **86**:69–92 (2003). doi:10.1016/S0168-3659(02)00321-8.
21. T. F. Wang, G. B. Kasting, and J. M. Nitsche. A multiphase microscopic diffusion model for stratum corneum permeability. I. formulation, solution, and illustrative results for representative compounds. *J. Pharm. Sci.* **95**:620–648 (2006). doi:10.1002/jps.20509.
22. M. Heisig, R. Lieckfeldt, G. Wittum, G. Mazurkevich, and G. Lee. Non steady-state descriptions of drug permeation through stratum corneum. I. The biphasic brick-and-mortar model. *Pharm. Res.* **13**:421–426 (1996). doi:10.1023/A:1016048710880.
23. A. Naegel, S. Hansen, D. Neumann, C. M. Lehr, U. F. Schaefer, G. Wittum, and M. Heisig. In-silico model of skin penetration based on experimentally determined input parameters. Part II: Mathematical modelling of *in-vitro* diffusion experiments. Identification of critical input parameters. *Eur. J. Pharm. Biopharm.* **68**:368–379 (2008). doi:10.1016/j.ejpb.2007.05.018.
24. G. C. Charalambopoulou, P. Karamertzanis, E. S. Kikkinides, A. K. Stubos, N. K. Kanellopoulos, and A. T. Papaioannou. A study on structural and diffusion properties of porcine stratum corneum based on very small angle neutron scattering data. *Pharm. Res.* **17**:1085–1091 (2000). doi:10.1023/A:1026453628800.
25. W. J. Albery, and J. Hadgraft. Percutaneous absorption: theoretical description. *J. Pharm. Pharmacol.* **31**:129–139 (1979).
26. A. S. Michaels, S. K. Chandrasekaran, and J. E. Shaw. Drug permeation through human skin: theory and *in vitro* experimental measurement. *Am. Inst. Chem. Eng. J.* **21**:985–996 (1975).
27. R. J. Phillips, W. M. Deen, and J. F. Brady. Hindered transport in fibrous membranes and gels: effect of solute size and fiber configuration. *J. Colloid Interface Sci.* **139**:363–373 (1990). doi:10.1016/0021–9797(90)90110-A.
28. K. J. Packer, and T. C. Sellwood. Proton magnetic reosnance studies of hydrated stratum corneum. Part 2.—self diffusion. *J. Chem. Soc. Faraday Trans. II*. **74**:1592–1606 (1978). doi:10.1039/f29787401592.
29. T.-F. Wang, G. B. Kasting, and J. M. Nitsche. A multiphase microscopic diffusion model for stratum corneum permeability. II. Estimation of physicochemical parameters, and application to a large permeability database. *J. Pharm. Sci.* **96**:3024–3051 (2007). doi:10.1002/jps.20883.
30. A. E. Kalinin, A. V. Kajava, and P. M. Steinert. Epithelial barrier function: asembly and structural features of the cornified cell envelope. *BioEssays*. **24**:789–800 (2002). doi:10.1002/bies.10144.
31. P. J. Caspers, G. W. Lucassen, H. A. Bruining, and G. J. Puppels. Automated depth-scanning confocal microspectrometer for rapid *in-vivo* determination of water concentration profiles in human skin. *J. Raman Spectrosc.* **31**:813–818 (2000) doi:10.1002/1097-555(200008/09)31:8/9<813::AID-JRS573>3.0.CO;2-7.
32. K. Walkley. Bound water in stratum corneum measured by differential scanning calorimetry. *J. Invest. Dermatol.* **50**:225–227 (1972). doi:10.1111/1523-747.ep12627251.
33. J. R. Hansen, and W. Yellin. NMR and infrared spectroscopy studies of stratum corneum hydration. In H. H. G. Jellinek (ed.), *Water structure at the water–polymer interface*, Plenum, New York, 1972, pp. 19–28.
34. M. I. Foreman. A proton magnetic resonance study of water in human stratum corneum. *Biochim. Biophys. Acta*. **437**:599–603 (1976).
35. D. A. Van Hal, E. Jeremiasse, H. E. Junginger, F. Spies, and J. A. Bouwstra. Structure of fully hydrated human stratum corneum: A freeze-fracture electron microscopy study. *J. Invest. Dermatol.* **106**:89–95 (1996). doi:10.1111/1523-1747.ep12328031.
36. G. C. Charalambopoulou, T. A. Steriotis, T. Hauss, A. K. Stubos, and N. K. Kanellopoulos. Structural alterations of fully hydrated human stratum corneum. *Physica B: Condensed Matter* **350**:e603–e606 (2004).
37. P. V. Raykar, M.-C. Fung, and B. D. Anderson. The role of protein and lipid domains in the uptake of solutes by human stratum corneum. *Pharm. Res.* **5**:140–150 (1988). doi:10.1023/A:1015956705293.
38. J. M. Nitsche, T. F. Wang, and G. B. Kasting. A two-phase analysis of solute partitioning into the stratum corneum. *J. Pharm. Sci.* **95**:649–666 (2006). doi:10.1002/jps.20549.
39. T. P. Banning, and C. M. Heard. Binding of doxycycline to keratin, melanin and human epidermal tissue. *Int. J. Pharm.* **235**:219–227 (2002). doi:10.1016/S0378-5173(01)00988-7.
40. C. M. Heard, B. V. Monk, and A. J. Modley. Binding of primaquine to epidermal membranes and keratin. *Int. J. Pharm.* **257**:237–244 (2003). doi:10.1016/S0378–5173(03)00140-6.
41. K. Kubota, E. Koyama, and E. H. Twizell. Dual sorption model for the nonlinear percutaneous permeation kinetics of timolol. *J. Pharm. Sci.* **82**:1205–1208 (1993). doi:10.1002/jps.2600821204.

42. C. Surber, K.-P. Wilhelm, M. Hori, H. I. Maibach, and R. H. Guy. Optimization of topical therapy: partitioning of drugs into stratum corneum. *Pharm. Res.* **7**:1320–1324 (1990). doi:10.1023/A:1015958526423.
43. C. Surber, K.-P. Wilhelm, H. I. Maibach, L. L. Hall, and R. H. Guy. Partitioning of chemicals into human stratum corneum: Implications for risk assessment following dermal exposure. *Fundam. Appl. Toxicol.* **15**:99–107 (1990). doi:10.1016/0272-0590(90)90167-I.
44. U. Hagedorn-Leweke, and B. C. Lippold. Accumulation of sunscreens and other compounds in keratinous substrates. *Eur. J. Pharm. Biopharm.* **46**:215–221 (1998). doi:10.1016/S0939-6411(97)00165-3.
45. H. Wagner, K. H. Kostka, C. M. Lehr, and U. F. Schaefer. Correlation between stratum corneum/water-partition coefficient and amounts of flufenamic acid penetrated into the stratum corneum. *J. Pharm. Sci.* **91**:1915–1921 (2002). doi:10.1002/jps.10183.
46. P. Meares. The diffusion of gases through polyvinyl acetate. *J. Am. Chem. Soc.* **76**:3415–3422 (1954). doi:10.1021/ja01642a015.
47. S. K. Chandrasekaran, P. S. Campbell, and T. Watanabe. Application of the "dual sorption" model to drug transport through skin. *Polym. Eng. Sci.* **20**:36–39 (1980). doi:10.1002/pen.760200107.
48. S. Hansen, A. Henning, A. Naegel, M. Heisig, G. Wittum, D. Neumann, K. H. Kostka, J. Zbytovska, C. M. Lehr, and U. F. Schaefer. In-silico model of skin penetration based on experimentally determined input parameters. Part I: Experimental determination of partition and diffusion coefficients. *Eur. J. Pharm. Biopharm.* **68**:352–367 (2008). doi:10.1016/j.ejpb.2007.05.012.
49. S. Mitragotri. A theoretical analysis of permeation of small hydrophobic solutes across the stratum corneum based on scaled particle theory. *J. Pharm. Sci.* **91**:744–752 (2002). doi:10.1002/jps.10048.
50. B. D. Anderson, W. I. Higuchi, and P. V. Raykar. Heterogeneity effects on permeability–partition coefficient relationships in human stratum corneum. *Pharm. Res.* **5**:566–573 (1988). doi:10.1023/A:1015989929342.
51. R. L. Anderson, and J. M. Cassidy. Variation in physical dimensions and chemical composition of human stratum corneum. *J. Invest. Dermatol.* **61**:30–32 (1973). doi:10.1111/1523-1747.ep12674117.
52. K. Abdulmajed, C. M. Heard, C. McGuigan, and W. J. Pugh. Topical delivery of retinyl ascorbate co-drug. 2. Comparative skin tissue and keratin binding studies. *Skin Pharmacol. Physiol.* **17**:274–282 (2004). doi:10.1159/000081112.
53. D. C. Schwartzendruber, P. Wertz, and D. T. Downing. Evidence that the corneocyte has a chemically bound lipid envelope. *J. Invest. Dermatol.* **88**:709–713 (1987). doi:10.1111/1523-1747.ep12470383.
54. S. Sobue, K. Sekiguchi, and T. Nabeshima. Intracutaneous distributions of fluconazole, itraconazole, and griseofulvin in Guinea pigs and binding to human stratum corneum. *Antimicrob. Agents Chemother.* **48**:216–223 (2004). doi:10.1128/AAC.48.1.216-223.2004.
55. H. Takahashi. Problems with the topical antimycotics. *Jpn. J. Med. Mycol.* **35**:331–334 (1994).
56. S. P. Banks Schlegel, and C. C. Harris. Tissue-specific expression of keratin proteins in human esophageal and epidermal epithelium and their cultured keratinocytes. *Exp. Cell Res.* **146**:271–280 (1983). doi:10.1016/0014-4827(83)90129-5.
57. P. G. Chu, and L. M. Weiss. Keratin expression in human tissues and neoplasms. *Histopathology*. **40**:403–439 (2002). doi:10.1046/j.1365-2559.2002.01387.x.
58. J. Kubilus, M. J. MacDonald, and H. P. Baden. Epidermal proteins of cultured human and bovine keratinocytes. *Biochim. Biophys. Acta*. **578**:484–492 (1979).
59. Y. Katz, and J. M. Diamond. A method for measuring nonelectrolyte partition coefficients between liposomes and water. *J. Membr. Biol.* **17**:69–86 (1974). doi:10.1007/BF01870173.
60. Y. Katz, and J. M. Diamond. Nonsolvent water in liposomes. *J. Membr. Biol.* **17**:87–100 (1974). doi:10.1007/BF01870174.
61. E. Abignente, and P. de Caprariis. Flufenamic acid. In K. Florey (ed.), *Analytical profiles of drug substances*, Vol. 11, Academic, New York, London, 1982, p. 324.
62. OECD. *Test guideline 427: Skin Absorption: In Vivo Method*. OECD, Paris, 2004.
63. OECD. *Test guideline 428: Skin Absorption: In Vitro Method*. OECD, Paris, 2004.
64. M. E. Johnson, D. Blankschtein, and R. Langer. Evaluation of solute permeation through the stratum corneum: lateral bilayer diffusion as the primary transport mechanism. *J. Pharm. Sci.* **86**:1162–1172 (1997). doi:10.1021/js960198e.
65. A. L. Bunge, and R. L. Cleek. A new method for estimating dermal absorption chemical exposure: 2. Effect of molecular weight and octanol–water partitioning. *Pharm. Res.* **12**:88–95 (1995). doi:10.1023/A:1016242821610.
66. R. O. Potts, and R. H. Guy. Predicting skin permeability. *Pharm. Res.* **9**:663–669 (1992). doi:10.1023/A:1015810312465.
67. H. Wagner, K. H. Kostka, C. M. Lehr, and U. F. Schaefer. pH profiles in human skin: influence of two *in vitro* test systems for drug delivery testing. *Eur. J. Pharm. Biopharm.* **55**:57–65 (2003). doi:10.1016/S0939-6411(02)00125-X.
68. K. M. Hanson, M. J. Behne, N. P. Barry, T. M. Mauro, E. Gratton, and R. M. Clegg. Two-photon fluorescence lifetime imaging of the skin stratum corneum pH gradient. *Biophys. J.* **83**:1682–1690 (2002). doi:10.1016/S0006-3495(02)73936-2.
69. S. Yadav, N. G. Pinto, and G. B. Kasting. Thermodynamics of water interaction with human stratum corneum I: Measurement by isothermal calorimetry. *J. Pharm. Sci.* **96**:1585–1597 (2007). doi:10.1002/jps.20781.
70. H. Wagner, K. H. Kostka, C. M. Lehr, and U. F. Schaefer. Drug distribution in human skin using two different *in vitro* test systems: comparison with *in vivo* data. *Pharm. Res.* **17**:1475–1481 (2000). doi:10.1023/A:1007648807195.
71. A. M. Kligman, and E. Christophers. Preparation of isolated sheets of human stratum corneum. *Arch. Dermatol. Res.* **88**:702–705 (1963).
72. R. J. Scheuplein. *Molecular structure and diffusional processes across intact stratum corneum: Semi-Annual Report*. US Army Chemical Research and Development Laboratories, Edgewood Arsenal, MD, 1966.
73. A. Alonso, J. V. Da Silva, and M. Tabak. Hydration effects on the protein dynamics in stratum corneum as evaluated by EPR spectroscopy. *Biochim. Biophys. Acta*. **1646**:32–41 (2003).
74. I. H. Blank, J. Moloney, 3rd, A. G. Emslie, I. Simon, and C. Apt. The diffusion of water across the stratum corneum as a function of its water content. *J. Invest. Dermatol.* **82**:188–194 (1984). doi:10.1111/1523-1747.ep12259835.
75. G. Imokawa, H. Kuno, and M. Kawai. Stratum corneum lipids serve as a bound-water modulator. *J. Invest. Dermatol.* **96**:845–851 (1991). doi:10.1111/1523-1747.ep12474562.
76. T. Richter, C. Peuckert, M. Sattler, K. Koenig, I. Riemann, U. Hintze, K.-P. Wittern, R. Wiesendanger, and R. Wepf. Dead but highly dynamic—the stratum corneum is divided into three hydration zones. *Skin Pharmacol. Physiol.* **17**:246–257 (2004). doi:10.1159/000080218.
77. G. B. Kasting, N. D. Barai, T. F. Wang, and J. M. Nitsche. Mobility of water in human stratum corneum. *J. Pharm. Sci.* **92**:2326–2340 (2003). doi:10.1002/jps.10483.
78. M. U. Zubair, M. M. A. Hassan, and I. A. Al-Meshal. Caffeine. In K. Florey (ed.), *Analytical profiles of drug substances*, Vol. 15, Academic, London, 1986.
79. W. R. Vieth, and K. J. Sladek. A model for diffusion in a glassy polymer. *J. Colloid Sci.* **20**:1014–1033 (1965). doi:10.1016/0095-8522(65)90071-1.
80. M. Schaefer-Korting, U. Bock, W. Diembeck, H. J. Düsing, A. Gamer, E. Haltner-Ukomadu, C. Hoffmann, M. Kaca, H. Kamp, S. Kersen, M. Kietzmann, H. C. Korting, H.-U. Kraechter, C.-M. Lehr, M. Liebsch, A. Mehling, C. Mueller-Goymann, F. Netzlaff, F. Niedorf, M. K. Ruebbelke, U. F. Schaefer, E. Schmidt, S. Schreiber, H. Spielmann, A. Vuia, and M. Weimer. Reconstructed human epidermis for skin absorption testing: Results of the German validation study. Altern. Lab. Anim. **34**:283–294 (2006).
81. M. D. Barratt. Quantitative structure–activity relationships for skin permeability. *Toxicol. In Vitro*. **9**:27–37 (1995). doi:10.1016/0887-2333(94)00190-6.
82. P. S. Magee. Some novel approaches to modelling transdermal penetration and reactivity with epidermal proteins. In J. Devillers (ed.), *Comparative QSAR*, Taylor & Francis, London, 1998, pp. 137–168.
83. E. Jaeckle, U. F. Schaefer, and H. Loth. Comparison of effects of different ointment bases on the penetration of ketoprofen through heat-separated human epidermis and artificial lipid barriers. *J. Pharm. Sci.* **92**:1396–1406 (2002). doi:10.1002/jps.10398.
84. H. Fischer, I. Polikarpov, and A. F. Craievich. Average protein density is a molecular-weight-dependent function. *Protein Sci.* **13**:2825–2828 (2004). doi:10.1110/ps.04688204.